

Mixed layer mesoscales: a parameterization for OGCMs

V. M. Canuto et al.

Mixed layer mesoscales: a parameterization for OGCMs

V. M. Canuto^{1,2}, M. S. Dubovikov^{1,3}, M. Luneva⁴, C. A. Clayson⁴, and
A. Leboissetier^{1,5}

¹NASA, Goddard Institute for Space Studies, 2880 Broadway, New York, NY, 10025, USA

²Department Applied of Phys. and Math., Columbia University, New York, NY, 10027, USA

³Center for Climate Systems Research, Columbia University, New York, NY, 10025, USA

⁴Department of Meteorology, Florida State University, Tallahassee, Florida, 32306-4520, USA

⁵Department of Earth, Atmospheric and Planetary Sciences, MIT, Cambridge, Massachusetts, 02138, USA

Received: 19 September 2009 – Accepted: 8 April 2010 – Published: 29 April 2010

Correspondence to: V. M. Canuto (vcanuto@giss.nasa.gov)

Published by Copernicus Publications on behalf of the European Geosciences Union.

Title Page

Abstract

Introduction

Conclusions

References

Tables

Figures

⏪

⏩

◀

▶

Back

Close

Full Screen / Esc

Printer-friendly Version

Interactive Discussion

Abstract

We derive and assess a parameterization of the mixed layer vertical and horizontal mesoscale fluxes of an arbitrary tracer. The results, which are obtained by solving the mesoscale dynamic equations and contain no adjustable parameters, are expressed in terms of the large scale fields resolved by coarse resolution OGCMs (ocean global circulation models).

The new model can be put in the right perspective by considering the following. Thus far, the lack of a mixed layer mesoscale model that naturally satisfies the required boundary condition (the vertical flux must vanish at the surface), was remedied by extending the stream function modeled for the adiabatic deep ocean into the mixed layer using an arbitrary tapering function chosen to enforce the required boundary condition. The present model renders the tapering schemes unnecessary for the vertical flux automatically vanishes at the ocean surface. The expressions we derive for the vertical and horizontal mesoscale fluxes are algebraic and should be used in conjunction with any of the available mesoscale models valid in the adiabatic deep ocean.

We also discuss a new feature representing the effect of sub-mesoscales on mesoscales. It is shown that in the case of strong wind, one must add to the mean Eulerian velocity that enters the parameterization of the mesoscale fluxes a new term due to sub-mesoscales whose explicit form we work out.

The assessment of the model results is as follows. First, previous eddy resolving results indicated a robust re-stratification effect by mesoscales; we show that the model result for the mesoscale vertical flux leads to re-stratification (its second z-derivative is negative) and that it is of the same order of magnitude but opposite sign of the vertical flux by small scale turbulence, leading to a large cancellation. Second, since mesoscales act as a source of the eddy kinetic energy, we compare the predicted surface values vs. the Topex-Poseidon. Third, we carry out an eddy resolving simulation and assess both z-profile and magnitude of the model vertical flux against the simulation data. The tests yield positive results.

Mixed layer mesoscales: a parameterization for OGCMs

V. M. Canuto et al.

Title Page

Abstract

Introduction

Conclusions

References

Tables

Figures



Back

Close

Full Screen / Esc

Printer-friendly Version

Interactive Discussion



A more stratified mixed layer has implication for the oceanic absorption of heat and CO_2 , a feature whose implications on climate predictions we hope to explore in the future.

1 Introduction

Ocean mesoscales are large (few Rossby deformation radii, 20–80 km), long lived (\sim months), energetic ($K > K_{\text{mean flow}}$) and ubiquitous features that are often not resolved in Ocean Global Circulation Models (OGCMs), especially those used in climate studies. Thus, a parameterization of mesoscale fluxes for an arbitrary tracer (T, S, concentrations, etc.) is required in terms of the large scale, resolved fields.

In the deep adiabatic ocean, the main effect of mesoscales is represented by an eddy induced velocity (bolus velocity) that was found to largely cancel the Eulerian mean velocity. The improvements in the OGCMs predictions brought about by such a representation in lieu of the standard large horizontal diffusivity, are well documented.

By contrast, the representation of mesoscales in the mixed layer has been much less developed and yet numerical simulations (e.g., Oschlies, 2002) have shown that mesoscales re-stratify the mixed layer leading to a cancellation of the de-stratification induced by small scale turbulence, an important dynamical effect that must be accounted for in coarse resolution OGCMs.

The mesoscale models presently available are only valid in the largely adiabatic ocean *below the mixed layer* and are of three types: two heuristic models, one suggested by Gent and McWilliams (1990, GM), the other by Treguier et al. (1997, THL) and the non-heuristic one derived from the mesoscale dynamic equations (Canuto and Dubovikov, 2005, 2006, CD5,6) which can be shown to encompass both GM and THL models as limiting cases. In the deep, almost adiabatic ocean, it was found convenient to represent mesoscales in terms of an eddy induced (bolus) velocity, a *residual flux* and a *Redi-like diffusion*. If the bolus velocity, usually denoted $\mathbf{u}^+(z)$, is to represent baroclinic instabilities, its z-integral vanishes and, when expressed in terms of a

OSD

7, 873–917, 2010

Mixed layer mesoscales: a parameterization for OGCMs

V. M. Canuto et al.

Title Page

Abstract

Introduction

Conclusions

References

Tables

Figures

⏪

⏩

◀

▶

Back

Close

Full Screen / Esc

Printer-friendly Version

Interactive Discussion



streamfunction $\Psi(z)$, one has the relations (for a discussion of this point, see Killworth, 1997, 2001):

$$\int_{-H}^0 \mathbf{u}^+(z) dz = 0, \quad \mathbf{u}^+(z) = -\frac{\partial \Psi(z)}{\partial z}, \quad \Psi(0) = 0 \quad (1a)$$

The commonly used GM model of the stream function, $\Psi_{GM} = \kappa_M L$, where $L = -\nabla_H \bar{b} / N^2$ is the slope of the isopycnals, satisfies the last relation in Eq. (1a) only if the mesoscale diffusivity $\kappa_M(z)$ vanishes at the surface $z=0$, see Killworth (2001), Sect. 5 and Eq. (5.6). On the other hand, using the Global Drifter Program/Surface Velocity Program, Zhurbas and Oh (2003) derived the following relation valid $\kappa_M(0) = (1.02 \pm 0.13) r_d K^{1/2}(0)$, where r_d is the Rossby deformation radius and $K(0)$ is the surface eddy kinetic energy whose values can be found in the work of Scharffenberg and Stammer (2010).

The discrepancy is not surprising since the GM and THL models were not constructed for the diabatic mixed layer but for the adiabatic deep ocean and the problem just mentioned is an indication that such models cannot be taken to represent the mixed layer which thus remains to be modeled. To avoid imposing the unphysical condition $\kappa_M(0)=0$, ad hoc tapering functions were introduced in the GM model so as to assure compliance with the last relation (Eq. 1a); the arbitrariness of the tapering functions is however of concern since the OGCMs results depend sensitively on the specific choice one makes (see Fig. 1 of Ferrari et al., 2008). A technical improvement over tapering procedures that attempt to connect the deep ocean directly to the mixed layer, was suggested (Ferrari et al., 2008) who introduced a transition layer between the two; the procedure is still phenomenological.

As Killworth (2005) first pointed out, since in the ML, especially in the vicinity of the surface, mixing does not occur along isopycnals, the most appropriate representation of the mesoscale fluxes is in terms of their horizontal and vertical components rather than in terms of a bolus velocity, residual flux and Redi diffusion which are more appropriate for the deep ocean where water parcels move mostly along isopycnal surfaces.

Mixed layer mesoscales: a parameterization for OGCMs

V. M. Canuto et al.

Title Page

Abstract

Introduction

Conclusions

References

Tables

Figures

⏪

⏩

◀

▶

Back

Close

Full Screen / Esc

Printer-friendly Version

Interactive Discussion



Discussion Paper | Discussion Paper | Discussion Paper | Discussion Paper | Discussion Paper

Therefore, in the mixed layer, we write the general dynamic equation for a mean arbitrary tracer that is used in coarse resolution OGCMs in the following way:

$$\partial_t \bar{\tau} + \bar{\mathbf{U}} \cdot \nabla \bar{\tau} + \nabla \cdot \mathbf{F}^m + \partial_z F_V^{ss} = G \quad (1b)$$

Here, G represents sources and sinks, $\mathbf{U}(=u, w)$ is the 3-D velocity field, $\mathbf{F}^m = \overline{\mathbf{U}'\tau'}$ is the 3-D mesoscale flux and $F_V^{ss} = -\partial_z(k_v \bar{\tau})$ is the small scale vertical flux. In the ocean interior, the vertical diffusivity k_v is small ($\approx 0.1 \text{ cm}^2 \text{ s}^{-1}$; Ledwell et al., 1993; Toole et al., 1994), while in the ML, k_v is strongly enhanced ($\approx 10^2 \text{ cm}^2 \text{ s}^{-1}$) resulting in a well mixed, de-stratified mixed layer.

In light of the above discussion, the goal of this work is the parameterization of the mesoscale flux $\mathbf{F}^m = \overline{\mathbf{U}'\tau'}$ in terms of resolved fields. We can anticipate that our model shows that the resulting F_V^m leads to a re-stratification since it has the opposite sign and similar magnitude of F_V^{ss} leading to a large cancellation.

The adiabatic GM, THL and CD5,6 formulations of the stream function $\Psi(z)$ should be used only below the mixed layer. The arbitrary tapering function is thus avoided and substituted with a new expression for the mesoscale fluxes we derive in this work which automatically satisfy the boundary condition that at $z=0$ the vertical mesoscale flux vanishes.

Both the tapering schemes and the approach by Ferrari et al. (2008) are phenomenological while we begin with the Langevin-type equations, which have a long tradition in non-linear problems, to describe the mesoscale fields. From the ensuing solutions we construct the second-order correlations that appear in Eq. (1b). The starting dynamic equations and thus the resulting fluxes in Eq. (1b), do not contain adjustable parameters. They are a generalization of the linearized equations of Killworth (1997, 2005) to include the non-linear terms which in turn are modeled using a turbulence closure developed and assessed in previous work. As discussed in CD5, the inclusion of non-linearities radically alters the solution of the equations. Specifically, while the linear equations of Killworth yielded eddies in the form of plane waves, the non-linear counterpart gives rise to a different picture of mesoscales which can be described as

Mixed layer mesoscales: a parameterization for OGCMs

V. M. Canuto et al.

Title Page

Abstract

Introduction

Conclusions

References

Tables

Figures



Back

Close

Full Screen / Esc

Printer-friendly Version

Interactive Discussion



“water-mass anomalies that have nearly circular flow around their centers which move through the background water at speeds and directions inconsistent with background flow”, in agreement with observations (Richardson, 1993).

Though the main result needed in Eq. (1b) is a parameterization of $\nabla \cdot \mathbf{F}^m$ itself, in order to use the mesoscale resolving simulation data to validate the mesoscale model, we shall use the flux itself $\mathbf{F}^m(\tau) = \overline{\mathbf{U}'\tau'}$ and use the following notation:

$$F_H = \overline{u'\tau'}, F_V = \overline{w'\tau'} \quad (1c)$$

The model results also predict an expression for the surface eddy kinetic energy which we show to compare well with the recent TOPEX-Poseidon data.

Finally, since recent studies (Levy et al., 2001, 2009; Thomas and Lee, 2005; Mahadevan, 2006; Mahadevan and Tandon, 2006; Klein et al., 2008; Thomas et al., 2008; Capet et al., 2008; Mahadevan et al., 2010), have shown that mixed layer dynamics is also strongly affected by sub-mesoscales $O(\leq 1 \text{ km})$, the latter must also be considered so as to have a complete model that includes both mesoscales and sub-mesoscales. In a previous paper (Canuto and Dubovikov, 2009), we presented a parameterization of the sub-mesoscale fluxes to be used in OGCMs that do not resolve sub-mesoscales but which resolve mesoscales. In a follow-up paper (Canuto and Dubovikov, 2010), we worked the extension of the latter to be used in OGCMs that do not resolve either mesoscales or sub-mesoscales, such as ones used in climate studies. Adding the meso and sub-mesoscales fluxes in the equation for the mean tracer (Eq. B3), is however not sufficient. In Sect. 2.7 we discuss a new effect representing the interaction of sub-mesoscales on mesoscale dynamics. The effect is accounted for by substituting the Eulerian mean velocity $\bar{\mathbf{u}}$ that appears in the parameterization of the sub-mesoscale fluxes with (see Appendix B):

$$\bar{\mathbf{u}} \rightarrow \bar{\mathbf{u}} + \mathbf{u}_{SM}^+ \quad (1d)$$

where the explicit form of the sub-mesoscale velocity \mathbf{u}_{SM}^+ is discuss in Sect. 2.7.

The organization of the paper is as follows. In Sect. 2.1, we derive the mesoscale tracer equation; in Sect. 2.2, we derive the expression for the mesoscale tracer field;

Mixed layer mesoscales: a parameterization for OGCMs

V. M. Canuto et al.

Title Page

Abstract

Introduction

Conclusions

References

Tables

Figures

⏪

⏩

◀

▶

Back

Close

Full Screen / Esc

Printer-friendly Version

Interactive Discussion



Mixed layer mesoscales: a parameterization for OGCMs

V. M. Canuto et al.

Title Page

Abstract

Introduction

Conclusions

References

Tables

Figures

◀

▶

◀

▶

Back

Close

Full Screen / Esc

Printer-friendly Version

Interactive Discussion



in Sect. 2.3 we derive the expression for the horizontal tracer flux; in Sect. 2.4 we derive the expression for the vertical mesoscale tracer flux; in Sect. 2.5 we derive the expression for the mesoscale kinetic energy; in Sect. 2.6 we discuss the necessity of filtering out inertial gravity waves from large scale fields; in Sect. 2.7 we discuss the effect of sub-mesoscales on the mesoscale flux; in Sect. 2.8 we discuss the matching conditions between the mixed layer and the interior; in Sect. 3.1 we discuss the de-stratification induced by small scale turbulence vs. the re-stratification induced by mesoscales; in Sect. 3.2 we present the comparison between the model results for the surface eddy kinetic energy and the Topex/Poseidon data; in Sect. 4.1 we discuss the eddy resolving simulation and the assessment of the model on that basis; in Sect. 5 we compare the contributions of mesoscales and sub-mesoscales to the vertical buoyancy flux; finally, in Sect. 6 we present some conclusions.

2 Dynamical mesoscale model in the ML and mesoscale tracer flux

2.1 Mesoscale tracer equation

Following standard procedure, the equation for the mesoscale tracer field is obtained by subtracting the averaged tracer equation from the equation for the full tracer. The result is:

$$\partial_t \tau' + \bar{\mathbf{U}} \cdot \nabla \tau' + \mathbf{U}' \cdot \nabla \bar{\tau} + Q_H^{\tau'} + Q_V^{\tau'} = \partial_z (k_V \partial_z \tau') \quad (2a)$$

where $Q_{H,V}^{\tau'}$ represent the non-linear terms;

$$Q_H^{\tau'} \equiv \mathbf{u}' \cdot \nabla_H \tau' - \overline{\mathbf{u}' \cdot \nabla_H \tau'}, \quad Q_V^{\tau'} \equiv w' \tau'_z - \overline{w' \tau'_z} \quad (2b)$$

As expected, the average of Eq. (2a) yields identically zero. In Eq. (2a) no closure was used for $Q_{H,V}^{\tau'}$. We follow Killworth (2005, hereafter K5) who suggested that because

of the strong mixing in the ML, one can use the approximations $\bar{\tau}_z=0$, $\tau'_z=0$. Thus, Eq. (2a) simplifies to:

$$\partial_t \tau' + \bar{\mathbf{u}} \cdot \nabla_H \tau' + \mathbf{u}' \cdot \nabla_H \bar{\tau} + Q_H^\tau = 0 \quad (2c)$$

Next, we Fourier transform Eq. (2c) in horizontal planes and time. Following K5, we keep the same notation \mathbf{u}' , τ' for the mesoscale fields in the \mathbf{k} - ω space and assume that the mean fields $\bar{\mathbf{u}}$ and $\nabla_H \bar{\tau}$ are constant in time and horizontal coordinates when Eq. (2c) is Fourier transformed. Under these conditions, the double Fourier transform of Eq. (2c) reduces to the formal substitution $\nabla_H \rightarrow i\mathbf{k}$, $\partial_t \rightarrow -i\omega$ when these operators act on mesoscale fields. Thus, we obtain:

$$i(\mathbf{k} \cdot \bar{\mathbf{u}} - \omega)\tau' + \mathbf{u}' \cdot \nabla_H \bar{\tau} + Q_H = 0 \quad (2d)$$

Without the non-linear term, this equation is equivalent to Eq. (2) of K5. We recall that τ' , \mathbf{u}' and the non-linear terms are functions of the horizontal wave vector \mathbf{k} , frequency ω and z while $\bar{\mathbf{u}}$ is a function of z only and $\nabla_H \bar{\tau}$ is z independent. Next, we apply the model for the non-linear terms Q_H developed in CD5. Though the complete expression is rather complex, it simplifies considerably in the vicinity of the maximum k_0 of the eddy energy spectrum $E(k)$. Additional simplifications are possible if the turbulent Prandtl number is taken to be $\sigma_t=1$ instead of the theoretical value $\sigma_t=0.72$. Then, from Eqs. (4e) and (8a,b) of CD5 we have:

$$Q_H(\mathbf{k}, \omega) = \chi \tau'(\mathbf{k}, \omega), \quad \chi = k_0 K^{1/2}, \quad K = \frac{1}{2} |\mathbf{u}'|^2 \quad (2e)$$

where, unlike Eq. (2d), \mathbf{u}' is taken in physical space and $\ell = k_0^{-1}$ is the mesoscale length scale which, outside the Tropics, equals the Rossby deformation radius.

Equation (2d) together with Eq. (2e), represent a stochastic Langevin equation. The advantage of the Langevin equation is that it is linear in the fluctuating fields and thus allows one to compute second-order moments while the original Eqs. (2d) and (2b), are highly non-linear and do not allow an analytical computation of such correlation

Mixed layer mesoscales: a parameterization for OGCMs

V. M. Canuto et al.

Title Page

Abstract

Introduction

Conclusions

References

Tables

Figures

⏪

⏩

◀

▶

Back

Close

Full Screen / Esc

Printer-friendly Version

Interactive Discussion



**Mixed layer
mesoscales: a
parameterization for
OGCMs**

V. M. Canuto et al.

Title Page

Abstract

Introduction

Conclusions

References

Tables

Figures

⏪

⏩

◀

▶

Back

Close

Full Screen / Esc

Printer-friendly Version

Interactive Discussion



functions. The problem is to find a model for the non-linear terms (Eq. 2b) which leads to a Langevin equation whose correlation functions are sufficiently close to those of the original Eqs. (2d) and (2b). This is the closure problem for the non-linear terms. In CD5, we used the closure derived by Canuto and Dubovikov (1997) and solved the eigenvalue problem to which the mesoscale dynamic equations were shown to reduce, resulting in Eq. (2e). Closure Eq. (2e) has a simple interpretation within the mixing length approach. Indeed, the first term is the standard relation with χ^{-1} being the characteristic time scale while the second and third relations, containing the characteristic length scale and velocity, are the only possible combinations that lead to a time scale. However, while in the framework of the mixing length approach, the second relation of Eq. (2e) has an undetermined coefficient, in the CD model such coefficient is no longer arbitrary.

2.2 Mesoscale tracer field

Substituting Eq. (2e) into the tracer Eq. (2d), we obtain that in the vicinity of $|\mathbf{k}|=k_0$, the expression for the mesoscale tracer field is given by:

$$\tau' = - \frac{\mathbf{u}' \cdot \nabla_H \bar{\tau}}{\chi + i(\mathbf{k} \cdot \bar{\mathbf{u}} - \omega)} \quad (3a)$$

Even though in principle in the Fourier transform leading to Eqs. (2d) and (3a), the variables ω and k are independent, the solution of the complete system of mesoscale equations in CD5 (which reduces to the eigenvalue problem mentioned above) yields the dispersion relation:

$$\omega(\mathbf{k}) = \mathbf{k} \cdot \mathbf{u}_d \quad (3b)$$

which has a simple interpretation. In fact, it coincides with the Doppler transformation for the frequency provided that in the system of coordinates moving with the velocity \mathbf{u}_d , the mesoscale flow is stationary, i.e., in this system $\omega=0$. In other words, Eq. (3b)

implies that \mathbf{u}_d is the *eddy drift velocity* i.e. mesoscale eddies are nothing but “water-mass anomalies that have nearly circular flow around their centers which move through the background water at speeds and directions inconsistent with background flow”, in agreement with observations (Richardson, 1993). The expression for \mathbf{u}_d in terms of mean fields is given in Eq. (4f) of CD6. With $\sigma_t=1$, it is given by:

$$\mathbf{u}_d = \langle \bar{\mathbf{u}} \rangle - \frac{1}{2} f r_d^2 \mathbf{e}_z \times \langle \partial_z L \rangle + \frac{1}{2} \mathbf{c}_R, \quad L = -\nabla_H \bar{b} / N^2 \quad (3c)$$

where \mathbf{e}_z is the unit vertical vector, L is the slope of isopycnal surfaces, \mathbf{c}_R is the velocity of the barotropic Rossby waves with the wave-vector directed along the x-axis and equal to r_d^{-1} :

$$\mathbf{c}_R = r_d^2 \mathbf{e}_z \times \boldsymbol{\beta}, \quad \boldsymbol{\beta} = \nabla f \quad (3d)$$

where f is the Coriolis parameter. In Eq. (3c), the bracket averaging is defined as follows:

$$\langle \cdot \rangle \equiv \int_{-H}^0 \cdot K^{1/2}(z) dz / \int_{-H}^0 K^{1/2}(z) dz \quad (3e)$$

where H is the ocean depth. Thus, solution (Eq. 3a) may be rewritten in terms of velocity fields only as follows:

$$\tau' = - \frac{\mathbf{u}' \cdot \nabla_H \bar{\tau}}{\chi + i \mathbf{k} \cdot (\bar{\mathbf{u}} - \mathbf{u}_d)} \quad (3f)$$

Relation (Eq. 3b) implies that the dependence of the mesoscale fields on ω is of the form:

$$A'(\omega, \mathbf{k}) = A'(\mathbf{k}) \delta(\omega - \mathbf{k} \cdot \mathbf{u}_d) \quad (3g)$$

Therefore, in (t, \mathbf{k}) -space the fields A' depend on time as follows:

$$A'(t, \mathbf{k}) = A'(\mathbf{k}) \exp(-i \mathbf{k} \cdot \mathbf{u}_d t) \quad (3h)$$

Mixed layer mesoscales: a parameterization for OGCMs

V. M. Canuto et al.

Title Page

Abstract

Introduction

Conclusions

References

Tables

Figures

⏪

⏩

◀

▶

Back

Close

Full Screen / Esc

Printer-friendly Version

Interactive Discussion



and we may interpret Eq. (3f) as a relation between the mesoscale fields τ' and u' in both (ω, \mathbf{k}) - and (t, \mathbf{k}) -spaces (recall that we denote mesoscale fields in different spaces by the same symbol).

2.3 Horizontal tracer flux

5 The general strategy to derive bilinear correlation functions of mesoscale fields such as the mesoscale fluxes, was developed by Killworth (1997) for the linearized case and in CD5 for the non-linear case. It consists of computing the functions in (t, \mathbf{k}) -space which, in the approximation of homogenous and stationary mean flow, have the form:

$$\overline{A'(t, \mathbf{k}')B'^*(t, \mathbf{k})} = \overline{A'B'^*(\mathbf{k})}\delta(\mathbf{k} - \mathbf{k}') \quad (4a)$$

10 which, because of Eq. (3h), does not depend on t . The function $Re(\overline{A'B'^*(\mathbf{k})})$ is called the density of $\overline{A'B'}$ in \mathbf{k} -space. The spectrum of the correlation function $\overline{A'B'}$ is then given by:

$$\overline{A'B'}(k) = \int Re \overline{A'B'^*(\mathbf{k})}\delta(k - |\mathbf{k}|)d^2\mathbf{k} \quad (4b)$$

i.e., the spectrum is obtained by averaging $Re \overline{A'B'^*(\mathbf{k})}$ over the directions of \mathbf{k} and multiplying the result by πk . Finally, the correlation function $\overline{A'B'}$ in physical space is obtained by integrating its spectrum.

15 In order to compute the horizontal tracer flux F_H in accordance with the above strategy, we begin by computing its density in \mathbf{k} -space:

$$F_H(\mathbf{k}) = Re \overline{u'\tau'^*(\mathbf{k})} \quad (4c)$$

20 where, in accordance with Eq. (4a), we have:

$$Re \overline{u'(t, \mathbf{k})\tau'^*(t, \mathbf{k}')} = Re \overline{u'\tau'^*(\mathbf{k})}\delta(\mathbf{k} - \mathbf{k}') \quad (4d)$$

Substituting Eq. (3f), we obtain:

$$F_H(\mathbf{k}) = -\frac{\chi}{\chi^2 + [\mathbf{k} \cdot (\bar{\mathbf{u}} - \mathbf{u}_d)]^2} \overline{u'_i u'^*_j}(\mathbf{k}) \cdot \nabla_H \bar{\tau} \quad (4e)$$

Since $|\mathbf{u}_d| \sim |\bar{\mathbf{u}}|$ and K exceeds the kinetic energy of the mean flow, using the second relation in Eq. (2e), we may neglect the second term in the denominator. Then, the first factor on the rhs of Eq. (4e) reduces to χ^{-1} . Next, carrying out the integration described in Eq. (4b) with Eq. (4e), we obtain:

$$\int \overline{u'_i u'^*_j}(\mathbf{k}) \delta(k - |\mathbf{k}|) d^2 \mathbf{k} = \frac{1}{2} \delta_{ij} \int |\mathbf{u}'|^2(\mathbf{k}) \delta(k - |\mathbf{k}|) d^2 \mathbf{k} = \delta_{ij} E(k) \quad (4f)$$

where $E(k)$ is the energy spectrum. Thus, from Eq. (4e), we obtain that the spectrum of the horizontal flux has the following form:

$$F_H(k) = -\chi^{-1} E(k) \nabla_H \bar{\tau} \quad (4g)$$

Integrating over k and assuming that the shapes of the spectra are similar, using the second relation in Eq. (2e), we finally derive that:

$$F_H = -\kappa_M \nabla_H \bar{\tau}, \quad \kappa_M = r_d K^{1/2} \quad (4h)$$

Thus, in the ML the horizontal tracer flux is given by a down-gradient diffusion with the diffusivity κ_M similar to that in the deep ocean (CD5,6) where on the other hand the down-gradient diffusion takes place along isopycnal rather than horizontal surfaces as in Eq. (4h). We note that using data from the Global Drifter Program/Surface Velocity Program, Zhurbas and Oh (2003) derived a surface diffusivity of the form $\kappa_M = C r_d K^{1/2}$ with $C=1.02 \pm 0.13$, a result that confirms Eq. (4h) (the result is valid outside the Tropics).

Mixed layer mesoscales: a parameterization for OGCMs

V. M. Canuto et al.

Title Page

Abstract

Introduction

Conclusions

References

Tables

Figures

⏪

⏩

◀

▶

Back

Close

Full Screen / Esc

Printer-friendly Version

Interactive Discussion



2.4 Vertical tracer flux

We begin by deriving the expression for the z-derivative of the vertical tracer flux

$$\partial_z F_v = \overline{w' \partial_z \tau'} + \overline{\tau' \partial_z w'} \quad (5a)$$

which enters the mean tracer Eq. (1b). Notice that Eq. (5a) is contributed only by the a-geostrophic component \mathbf{u}_a of the eddy velocity. In particular, the second term can be rewritten as follows:

$$\overline{\tau' \partial_z w'} = - \overline{\tau' \nabla_H \cdot \mathbf{u}'} = - \overline{\tau' \nabla_H \cdot \mathbf{u}_a} \quad (5b)$$

In order to compute this correlation function, we follow the procedure described in the beginning of Sect. 2.3 and consider the corresponding density in \mathbf{k} space where $\mathbf{u}_a = (\mathbf{k}/k) u_a$. Thus, we have

$$Re \overline{\tau'^* \partial_z w'}(k) = Re \left(-ik \overline{u_a \tau'^*}(k) \right) = k \text{Im} \overline{u_a \tau'^*}(k) \quad (5c)$$

The relation between eddy geostrophic and a-geostrophic components in the ML differs from that in the adiabatic ocean, Eq. (10a) of CD5, by the sign of the dynamical viscosity ν . In fact, as we showed in CD5, in the adiabatic regime the enstrophy cascade cannot occur since the non-linear interactions do not conserve enstrophy. For this reason, there is only an inverse kinetic energy cascade (in wave number space) which entails a negative dynamical viscosity. Near the surface, enstrophy is conserved by non-linear interactions and this allows an enstrophy cascade which results in a positive turbulent viscosity. As a result, in the ML, in Eq. (10a) of CD5 we must change the sign of ν . In addition, since we adopt the turbulent Prandtl number $\sigma_t = 1$, we have $\tilde{\nu} = \tilde{\chi}$. Using relation Eq. (10a) of CD5 with the opposite sign of $\tilde{\nu}$ and the continuity equation, we obtain (for simplicity we omit the tilde):

$$w'_z = -ik u_a = kf^{-1} [\mathbf{k} \cdot (\bar{\mathbf{u}} + \mathbf{c}_R - \mathbf{u}_d) - i\chi] u_a \quad (5d)$$

Title Page

Abstract

Introduction

Conclusions

References

Tables

Figures

⏪

⏩

◀

▶

Back

Close

Full Screen / Esc

Printer-friendly Version

Interactive Discussion



where \mathbf{u}_g is the geostrophic component of the eddy velocity. Next, we substitute Eq. (5d) and Eq. (3f) into Eq. (5c) and take into account that for mesoscales $u_a \ll u_g$ and therefore $\mathbf{u}' \approx \mathbf{u}_g = \mathbf{n} \times \mathbf{e}_z u_g$ where $\mathbf{n} = \mathbf{k}/|\mathbf{k}|$. We obtain:

$$Re \overline{\tau' \partial_z w'}(\mathbf{k}) = -2(\chi f)^{-1}(\bar{\mathbf{u}} - \mathbf{u}_d + \frac{1}{2}\mathbf{c}_R) \cdot \mathbf{k} \mathbf{k} \times \mathbf{e}_z \cdot \nabla_H \bar{\tau} |u_g|^2(\mathbf{k}) \quad (6a)$$

5 To derive the corresponding relation for the spectra, we substitute Eq. (6a) into Eq. (4b) that reduces to averaging over directions of \mathbf{k} . Taking into account that the average of the tensor $k_i k_j$ yields $\delta_{ij} |\mathbf{k}|^2 / 2$ where $|\mathbf{k}| \approx k_0 = r_d^{-1}$, and that the spectrum of $|u_g|^2$ equals $2E(k)$, we obtain:

$$\overline{\tau' \partial_z w'}(k) = -2(\chi f r_d^2)^{-1}(\bar{\mathbf{u}} - \mathbf{u}_d + \frac{1}{2}\mathbf{c}_R) \times \mathbf{e}_z \cdot \nabla_H \bar{\tau} E(k) \quad (6b)$$

10 Assuming that the shape of the spectra in the right and left hand sides are similar, we integrate over k which reduces to a substitution of the spectra with the corresponding variables. In addition, we use the second relations in Eqs. (2e) and (4h) to obtain:

$$\overline{\tau' \partial_z w'} = -2 \kappa_M (f r_d^2)^{-1}(\bar{\mathbf{u}} - \mathbf{u}_d + \frac{1}{2}\mathbf{c}_R) \times \mathbf{e}_z \cdot \nabla_H \bar{\tau} \quad (6c)$$

15 Next, we compute the first term of Eq. (5a). To do so, we need the expressions for $w'(t, \mathbf{k})$ and $\tau'_z(t, \mathbf{k})$. The former function can be derived by integrating Eq. (5d). With accuracy to the main order in z , we obtain:

$$w' = z k f^{-1} [\mathbf{k} \cdot (\hat{\mathbf{u}} + \mathbf{c}_R - \mathbf{u}_d) - i \chi] u_g, \quad z \hat{\mathbf{u}}(z) = \int_0^z \bar{\mathbf{u}}(z') dz' \quad (7a)$$

since $\chi = r_d K^{1/2}$ and $u_g \approx K^{1/2}$ are almost constant within the ML. Differentiating Eq. (3f) under the same condition, we get:

$$20 \quad \tau'_z \approx i \chi^{-2} \mathbf{k} \cdot \bar{\mathbf{u}}_z (\mathbf{u}' \cdot \nabla_H \bar{\tau}) \quad (7b)$$

Mixed layer mesoscales: a parameterization for OGCMs

V. M. Canuto et al.

Title Page	
Abstract	Introduction
Conclusions	References
Tables	Figures
◀	▶
◀	▶
Back	Close
Full Screen / Esc	
Printer-friendly Version	
Interactive Discussion	



Using Eq. (7a,b) to compute $Re \overline{w' \partial_z \tau'^*}(\mathbf{k})$ and using a procedure analogous to Eq. (6a–c), we derive:

$$\overline{w' \partial_z \tau'} = z \kappa_M (f r_d^2)^{-1} \mathbf{e}_z \times \overline{\mathbf{u}}_z \cdot \nabla_H \overline{\tau} \quad (7c)$$

Summing Eqs. (7c) and (6c) and substituting into Eq. (5a), with account for Eq. (3c), we get:

$$\partial_z F_V^0 \equiv \partial_z \overline{w' \tau'} = \mathbf{u}_* \cdot \nabla_H \overline{\tau} \quad (8a)$$

$$\mathbf{u}_* = z \phi_M \mathbf{e}_z \times \overline{\mathbf{u}}_z - [\kappa_M \langle \partial_z L \rangle + 2 \phi_M \mathbf{e}_z \times (\langle \overline{\mathbf{u}} \rangle - \overline{\mathbf{u}})], \quad \phi_M = \frac{\kappa_M}{f r_d^2} \quad (8b)$$

and \mathbf{u}_* may be viewed as a 2-D eddy induced velocity in the ML. The superscript 0 in Eq. (8a) is a reminder that the result is obtained in the approximation $\overline{\tau}_z = 0$ which has been adopted throughout the above analysis starting with Eq. (2c). Therefore, in order to make \mathbf{u}_* the analog of the eddy induced velocity in the ocean interior, we may add the term $w_* \overline{\tau}_z$ to the rhs of Eq. (8a).

However, in the vicinity of the lower boundary of the ML, such an approximation is insufficient for the computation of $\overline{w' \tau'}$ and $\partial_z \overline{w' \tau'}$. Thus, we need to account for a correction $\delta \tau'$ to Eq. (3f) due to a non-zero $\overline{\tau}_z$ which we compute in Appendix A where we show that the correction results in the following additional term to the vertical flux:

$$\delta F_V = -\kappa_V \frac{\partial \overline{\tau}}{\partial z}, \quad \kappa_V = 2 z^2 f \phi_M^3 \quad (8c)$$

The corresponding correction to the z-derivative (Eq. 8a) is mostly contributed by the differentiation of $\overline{\tau}_z$ in Eq. (8c). Thus, we have:

$$\partial_z \delta F_V = -\kappa_V \partial_{zz} \overline{\tau} \quad (8d)$$

Integrating Eqs. (8a,b) over z and adding Eq. (8c), one obtains the final form of the mesoscale vertical flux of an arbitrary tracer (see definition in Eq. 1c):

$$F_V = -\kappa_H \cdot \nabla_H \overline{\tau} - \kappa_V \partial_z \overline{\tau}, \quad (9a)$$

Mixed layer mesoscales: a parameterization for OGCMs

V. M. Canuto et al.

Title Page

Abstract

Introduction

Conclusions

References

Tables

Figures

◀

▶

◀

▶

Back

Close

Full Screen / Esc

Printer-friendly Version

Interactive Discussion



where:

$$\kappa_H = \kappa_M z [F_1 - F_2(z)] \quad (9b)$$

$$F_1 = \langle \partial_z L \rangle + 2f^{-1} r_d^{-2} \mathbf{e}_z \times \langle \bar{\mathbf{u}} \rangle \quad (9c)$$

$$F_2(z) = f^{-1} r_d^{-2} \mathbf{e}_z \times (2 \hat{\mathbf{u}} + \frac{1}{2} z \partial_z \bar{\mathbf{u}}) \quad (9d)$$

- 5 where $\hat{\mathbf{u}}$, $\langle \cdot \rangle$, κ_V , κ_M and \mathbf{L} are defined in Eqs. (7a), (3e), (8c), (4h) and (3c). The function \mathbf{F}_1 is z-independent and proportional to a weighted mean over the ocean's interior and represents the effect of the abyssal ocean on the vertical flux in the ML.

2.5 Mesoscale kinetic energy in terms of large scale fields

10 The last variable we need to model is the mesoscale kinetic energy K in terms of large scale fields. To that end, we recall that the K -equation, Eq. (2a) in CD6, shows that the vertical buoyancy flux F_V^b is a source of K . Assuming that the production P_K of mesoscale kinetic energy occurs at scales ℓ , we use the relations:

$$K^{3/2} = C \ell P_K, \quad (10a)$$

$$P_K = \langle F_V^b \rangle \equiv h^{-1} \int_{-h}^0 F_V^b dz \quad (10b)$$

- 15 Since P_K is a power, upon multiplying it by the dynamical time scale $\tau = 2K\varepsilon^{-1}$ one obtains an energy and then using $\varepsilon = \ell^{-1} K^{3/2}$, one derives Eq. (10a). A more basic justification can be found in the book on turbulence by Lesieur (1990). With the help of data from a mesoscale resolving simulation to be discussed in Sect. 4, we have validated Eq. (10a). It is worth noticing that a relation analogous to Eq. (10a) also
 20 applies to sub-mesoscales which we validated in CD9 using the simulation data of

Capet et al. (2008). The coefficient C is related to the Kolmogorov constant as follows $C=(3 Ko/2)^{3/2}$. Substituting Eqs. (9a–d) into Eq. (10a), we obtain

$$K = Ch\left(\frac{1}{2}r_d^2 F_1 + f^{-1}\mathbf{V} \times \mathbf{e}_z\right) \cdot \nabla_H \bar{\mathbf{b}} \quad (10c)$$

where:

$$\mathbf{V} = \frac{1}{2}\bar{\mathbf{u}}(z = -h) + \frac{2}{h}\int_{-h}^0 \bar{\mathbf{u}}dz + \frac{3}{h^2}\int_{-h}^0 \bar{\mathbf{u}}zdz \quad (10d)$$

Relations (Eqs. 10c,d) yield the mixed layer K in terms of mean fields. We notice that in addition to the non-trivial solution Eq. (10c), Eq. (10a) has the solution $K=0$ because we have cancelled $K^{1/2}$ after substituting Eqs. (9a,b) into Eq. (10a) since Eq. (9a) contains $\kappa_M = r_d K^{1/2}$. The zero solution is realized when the non-trivial one (Eq. 10c) is not positive. The physical interpretation is that in such cases mesoscale eddies are not generated.

2.6 Filtering large scale fields in coarse resolution OGCMs

When using relations Eqs. (4h), (8a,b), (10) to model unresolved mesoscales in the tracer Eq. (1b), one must keep in mind that such parameterization was derived using Eq. (2d) for the mesoscale tracer field τ' in which we assumed that the large scale fields $\bar{\mathbf{u}}$ and $\nabla\bar{\tau}$ are time independent. It is clear that in order to extend the applicability of the parameterization to the case of time dependent $\bar{\mathbf{u}}$ and $\nabla\bar{\tau}$, the characteristic time scale of the latter must exceed that of mesoscales which is of the order of 1 month. Moreover, instantaneous OGCMs fields also contain the contribution of inertial waves which have time scales shorter than 1 day and do not effect mesoscale eddies. Therefore, in order to use Eqs. (4h), (8a,b) and (10) in coarse resolution OGCMs, one must filter out wave fields from large scale ones by averaging the latter over sufficiently long times. Since there is a huge gap between the inertial time scale and that of the large scale flow

$\sim L / |\bar{\mathbf{u}}|$ (where L is a characteristic horizontal scale), which is in any case longer than its mesoscale counterpart, it is sufficient to average the instantaneous large scale fields over several days.

2.7 Effect of submesoscales on mesoscales

5 As discussed in the Introduction, the effects of meso and sub-mesoscales (SM, ≤ 1 km), are not simply additive. In Appendix B, we show that in the presence of a strong downfront wind, which is a case of great practical interest, one must add a new term to the left hand side of Eq. (2a) which has the following form:

$$\mathbf{u}_{\text{SM}}^+ \cdot \nabla_{\text{H}} \tau', \quad \mathbf{u}_{\text{SM}}^+ = -\eta(\tilde{\mathbf{u}} - \lambda \mathbf{e}_z \times \tilde{\mathbf{u}}) \quad (11a)$$

10 where we have introduced the following dimensionless variables:

$$\eta = x(1+x+y^2)^{-1}, \quad \lambda = yx^{1/2}(1+x)^{-1}, \quad x = \frac{K_{\text{SM}}}{\tilde{K}}, \quad y = \frac{r_{\text{S}} f}{\tilde{K}^{1/2}}, \quad r_{\text{S}} = \frac{Nh}{\pi|f|} \quad (11b)$$

and where:

$$\tilde{\mathbf{u}} = \bar{\mathbf{u}} - \langle \bar{\mathbf{u}} \rangle_{\text{ML}}, \quad \tilde{K} = \frac{1}{2} |\tilde{\mathbf{u}}|^2, \quad \langle \bar{\mathbf{u}} \rangle_{\text{ML}} = h^{-1} \int_{-h}^0 \bar{\mathbf{u}}(z) dz \quad (11c)$$

15 Here, r_{S} is the deformation radius in the ML of depth h , K_{SM} is sub-mesoscale eddy kinetic energy and \tilde{K} can be interpreted as the baroclinic mean kinetic energy. The variable x is obtained solving the equation:

$$\frac{1+x+y^2}{15.8 h_{\text{S}}} \tilde{K}^{3/2} x^{1/2} = \mathbf{V} \cdot \nabla_{\text{H}} b + \frac{yx^{1/2}}{1+x} \mathbf{V} \times \mathbf{e}_z \cdot \nabla_{\text{H}} b \quad (11d)$$

where:

$$\mathbf{V} = h^{-2} \int_{-h}^0 dz \int_z^0 \tilde{\mathbf{u}}(z') dz' \quad (11e)$$

Mixed layer mesoscales: a parameterization for OGCMs

V. M. Canuto et al.

Title Page

Abstract

Introduction

Conclusions

References

Tables

Figures

◀

▶

◀

▶

Back

Close

Full Screen / Esc

Printer-friendly Version

Interactive Discussion

3 Assessment of the mesoscale model

3.1 Re-stratification of the mixed layer by mesoscales

Taking the z-derivative of Eq. (1b) with $\bar{\tau}=\bar{b}$ and recalling that $\partial_z \bar{b}=N^2$, we have:

$$\frac{\partial N^2}{\partial t} = -\frac{\partial^2 F_V}{\partial z^2} - \frac{\partial^2 F_V^{ss}}{\partial z^2} \dots \quad (13)$$

5 where for the present purposes we have kept only the vertical mesoscale flux. Clearly, whether mesoscales de-stratify or re-stratify the mixed layer depends on the sign of the z second derivative of the vertical flux F_V . Small scale turbulent vertical fluxes are known to de-stratify the ML, in the mesoscale case given by Eq. (9), the contribution of the F_1 in Eq. (9) is linear in z and thus F_1 does not contribute to the second derivative in Eq. (13). The term $F_2(z)$ is contributed by the large scale velocity in the ML whose profile varies considerably within the Ekman layer. Below the latter, $F_2(z)$ is geostrophic and we have $\partial_{zz} F_V = -3 f^{-1} \phi_M \left| \nabla_H \bar{b} \right|^2 < 0$ and thus, below the Ekman layer, mesoscales re-stratify the ML. Near the bottom of the ML, the contribution of δF_V given by Eq. (8c) to the re-stratification of the ML becomes important. The re-stratification of the mixed layer by mesoscales predicted by the present model is in accord with the conclusions of numerical simulations (Oschlies, 2002).

3.2 Surface kinetic energy vs. Topex/Poseidon data

We now compare the surface eddy kinetic energy K_S calculated from our model given by Eq. (10) with the observational Topex-Poseidon data of Scharffenberg and Stammer (2010) presented in Fig. 1a (the data are averaged over 3 years). Our model K_S is shown in Fig. 1b and was computed using the large scale fields obtained from a coarse $3^\circ \times 3^\circ$ OGCM (NCAR-CSM; Large et al., 1997) with a vertical mixing model with tides and double diffusion discussed elsewhere (Canuto et al., 2010). The K_S was

Mixed layer mesoscales: a parameterization for OGCMs

V. M. Canuto et al.

Title Page

Abstract

Introduction

Conclusions

References

Tables

Figures

⏪

⏩

◀

▶

Back

Close

Full Screen / Esc

Printer-friendly Version

Interactive Discussion



also averaged over 3 years after the OGCM reached equilibrium and the large scale fields were averaged over ten days, as discussed in Sect. 7. The model K_S exhibits the same structure and features of the data exhibiting the same intensity in the Gulf Stream and in the ACC. In order to further assess the comparison between the data and the OGCM run, we carried out the following statistical estimates. The root mean square of the surface K_S is calculated as:

$$K_s(\text{rms}) = \left(\frac{\sum \alpha_i K_{si}^2}{\sum \alpha_i} \right)^{1/2} \quad (14a)$$

where α_i is the area of the grid cell and weights the rms. Furthermore, in most places the difference $K_s(\text{data}) - K_s(\text{model})$ is found to be $\pm 50 \text{ cm}^2 \text{ s}^{-2}$. The RMS of K_S for the data and our model are $312 \text{ cm}^2 \text{ s}^{-2}$ and $313 \text{ cm}^2 \text{ s}^{-2}$ respectively, proving the model's ability to estimate K_S . The RMS difference:

$$K_s(\text{rms : data - model}) = \left(\frac{\sum \alpha_i [K_{si}(\text{data}) - K_{si}(\text{model})]^2}{\sum \alpha_i} \right)^{1/2} \quad (14b)$$

has a value of $199 \text{ cm}^2 \text{ s}^{-2}$. The correlation (data, model) is 0.58 and the covariance (data, model) is positive with a value of $16\,779 \text{ (cm}^2 \text{ s}^{-2})^2$.

4 Assessment of the mesoscale model with an eddy resolving simulation

To assess the parameterization of the horizontal and vertical mesoscale tracer fluxes (Eq. 4h), (Eqs. 9a–d) and mesoscale kinetic energy (Eqs. 10c,d), we carried out a mesoscale resolving simulation. The resolved fields allow us to find both fluctuating and mean fields and to diagnose the correlation functions (Eq. 1c) and the last of Eq. (2e) and then to test the parameterization relations (Eqs. 4h, 9a–d, and 10c,d).

Mixed layer mesoscales: a parameterization for OGCMs

V. M. Canuto et al.

Title Page

Abstract

Introduction

Conclusions

References

Tables

Figures

⏪

⏩

◀

▶

Back

Close

Full Screen / Esc

Printer-friendly Version

Interactive Discussion

4.1 Numerical experiments

We simulated two kinds of flows: (1) idealized flows driven by only baroclinic instabilities with no wind stress and surface fluxes, and (2) realistic flows with wind stresses and surface fluxes under conditions typical for the Sea of Japan (SOJ) with the circulation driven by inflow-outflow in shallow and narrow straits similar to the conditions of the Tsushima and Soya Straits. In Sect. 2.6, we showed that since resolved OGCMs instantaneous fields contain a mixture of inertial waves that do not contribute to the mean fields in Eqs. (4h), (9a–d) and (10), the mixture must be filtered out by averaging over several days. Of course, this conclusion remains valid in eddy resolving simulations which are used to diagnose mesoscale fluxes. However, the problems of diagnosing are not completely solved by filtering the mean fields. In fact, mesoscale fields in eddy resolving simulations are contained in the fluctuating components A' which are computed by subtracting the resolved fields averaged over a grid volume \bar{A} from the fields themselves, i.e., $A' = A - \bar{A}$. In addition to the mesoscale fields, the fluctuating fields contain sub-mesoscale and background fields with time scales less than one day, neither of which contributes to the mesoscale fluxes. Therefore, before computing the latter, the former must be filtered out by averaging the fluctuating fields over several days since the characteristic time scale of mesoscale fields is of the order of 1 month. Thus, together with the considerations in Sect. 2.6, when assessing the mesoscale parameterizations (Eqs. 4h, 9a–d, 10) using eddy resolving simulations, one must begin by filtering out fields with inertial time scales (of any length scale) by averaging over several days.

4.1.1 Numerical code

The numerical code we employ is based on the σ -coordinate modification of University of Colorado (CU) version of the sigma-coordinate free surface primitive equation Princeton Ocean Model (POM) originally developed by George Mellor's group

OSD

7, 873–917, 2010

Mixed layer mesoscales: a parameterization for OGCMs

V. M. Canuto et al.

Title Page

Abstract

Introduction

Conclusions

References

Tables

Figures

⏪

⏩

◀

▶

Back

Close

Full Screen / Esc

Printer-friendly Version

Interactive Discussion



Mixed layer mesoscales: a parameterization for OGCMs

V. M. Canuto et al.

Title Page

Abstract

Introduction

Conclusions

References

Tables

Figures

⏪

⏩

◀

▶

Back

Close

Full Screen / Esc

Printer-friendly Version

Interactive Discussion



at Princeton (Blumberg and Mellor, 1987). The curvilinear version of the model (the CUPOM), developed and documented by Kantha and Piacsek (1993, 1997) differs from the original POM by better mixed-layer parameterization (Kantha and Clayson, 1994, 2000; Kantha, 2003). The model was successfully applied at CU to nowcast/forecasts in the Gulf of Mexico (Choi et al., 1995; Kantha, 1999), the tropical Pacific (Clayson, 1995), the North Indian Ocean (Lopez, 1998; Lopez and Kantha, 2000), the North Pacific (Engelhardt, 1996) and the Sea of Japan (Suk and Kantha, 1997). The operational versions of the model are used at the Naval Oceanographic Office (NAVO) for the Mediterranean Sea (Horton et al., 1997), the Red Sea (Clifford et al., 1997), the Baltic Sea and the Persian Gulf (Horton et al., 1991, 1992). The σ -z version of CUPOM used in this study follows the structure of the sigma version. Some modifications were made in the scheme of integration of the continuity equation and the vertical velocity in order to satisfy the boundary conditions for the pseudo-vertical velocity at the surface and the vertical velocity at the bottom within machine accuracy (Clayson et al., 2008; Appendix B). The present model includes also recent developments in turbulence (Kantha, 2003) for the mixed layer mixing scheme. This modification was used in the eddy-resolving simulation of the Sea of Japan (Clayson and Luneva, 2004; Luneva and Clayson, 2006; Clayson et al., 2008). The model realistically describes upper and deep circulation, locations of fronts, seasonal variability and depth and location of the deep convection. The model was assessed against data on the spatial and seasonal variability from the satellite SST, surface buoys currents (Lee and Niiler, 2005), abyssal energy and currents from PALACE floats and mooring stations (Takematsu et al., 2005).

4.1.2 Idealized flows: baroclinic instabilities only

The simulations consist in solving an initial value problem of a decaying baroclinic instability with the initial mean buoyancy gradient chosen to be $(1, 2, 5) \cdot 10^{-9} \text{ s}^{-2}$. The buoyancy profiles were taken to be exponentially decaying with depth. We simulated flows in three rectangular basins (1×1 , 1.5×2 and 3×1.5) 10^3 km with a constant depth of

4 km. The Rossby radius varied from (30–50) km. The horizontal resolution is 0.07 degrees with a vertical resolution of 36 σ -z levels of which 12 are in the ML (the upper 100 m) with (5–10) m vertical grid size. The horizontal diffusivity-viscosity are modeled with a Smagorinsky operator with a horizon parameter of 0.07 and a background diffusivity/viscosity of (4–7) $\text{m}^2 \text{s}^{-1}$ depending on the grid size. The vertical diffusivity is $k_v=5 \cdot 10^{-3} \text{m}^2 \text{s}^{-1}$ in the ML and $k_v=10^{-5} \text{m}^2 \text{s}^{-1}$ below the ML. During the decay of the initial baroclinic instability, potential energy is released and transformed into kinetic energy. Depending on the initial conditions, the rate of transformation grows for the first 100–400 days and then stabilizes. For the next 100–200 days, the simulated flow contains plenty of eddies of (100–200) km size which hardly change for the period during which we analyzed flow fields and eddy fluxes. The instantaneous sea surface level and currents are shown in Fig. 2a–c for 3 different experiments. As we discussed above, before analyzing the eddy fluxes, we filtered out the inertial time scale fields by averaging them over 10 days. The typical values of the large scale velocity (averaged over the coarse grid size ~ 200 km) are (2–3) cm s^{-1} and (15–30) cm s^{-1} for the eddies.

4.1.3 Realistic flows: wind stresses and surface fluxes

We also simulated circulations driven by inflows and outflows through the western and eastern boundaries shown in Fig. 3a–b and by heat and momentum surface fluxes with strong seasonal, synoptic and diurnal variability but smoothed horizontally. The simulation domain is 800×10^3 km horizontal size, a depth around 3.6 km and the shallow inflow and outflow straits of 200 m depth, which are conditions similar to the Tsushima and Soya Straits in the Sea of Japan. The horizontal resolution is 4 km (2 km for several experiments with the Rossby radius smaller than 10 km) with 43 σ -z levels with a well-resolved upper 200 m (the corresponding grid size is 10 m). The zonally homogeneous initial temperature and salinity were taken from the ship observations in July–August 1999 in Sea of Japan along 134 E longitude. The simulation was spun up for five years with the annual repetition of the surface forcing from ECMWF for the period October 1999–October 2000 in the north-western part of the Sea of Japan. The

Mixed layer mesoscales: a parameterization for OGCMs

V. M. Canuto et al.

Title Page

Abstract

Introduction

Conclusions

References

Tables

Figures

⏪

⏩

◀

▶

Back

Close

Full Screen / Esc

Printer-friendly Version

Interactive Discussion



Mixed layer mesoscales: a parameterization for OGCMs

V. M. Canuto et al.

Title Page

Abstract

Introduction

Conclusions

References

Tables

Figures

⏪

⏩

◀

▶

Back

Close

Full Screen / Esc

Printer-friendly Version

Interactive Discussion



forcing is characterized by strong heat losses and strong winds in winter and weak winds and high solar radiation in late spring and summer. The resulting flow was taken as initial condition for additional three months simulations performed using the three month surface forcing in ECMWF for the period from 1 November 1999 to 1 February 2000 as the basic forcing. We performed about 70 numerical experiments with the surface forcing differing from the basic one by the factors from 0 to 2 for the wind stresses τ/τ_0 with $\tau_0=0.2\text{Nm}^{-2}$ and from 0 to 4 for the heat flux. As it is seen from two typical snapshots in Fig. 2a, the circulation consists of two main jets at the center of the basin and near the southern boundary with numerous eddies and weaker loop currents to the north of the main jet. Eddy sizes varied in the interval 30–100 km. Eddy velocity varied in the interval (20–40) cm s^{-1} while with the coarse grid (120×120) km the mean velocity is $\sim 7\text{--}10\text{ cm s}^{-1}$.

4.2 Results of simulations and testing the parameterization

4.2.1 Idealized flows

(a) Horizontal flux and diffusivity

As we discussed at the end of Sect. 2.3, the form of the diffusivity predicted by the present model, Eq. (4h), agrees with the result based on observations derived by Zhurbas and Oh (2003). Thus, the results for the horizontal diffusivity presented below may be considered a test of the numerical scheme rather than of the mesoscale model. Assuming the first relation of Eq. (4h) for the horizontal flux, we deduce the following expression for the diagnosed mesoscale diffusivity:

$$\kappa_M^d = - \frac{\overline{u'b'} \cdot \nabla_H \bar{b}}{\nabla_H \bar{b} \cdot \nabla_H \bar{b}} \quad (14c)$$

A feature of κ_M^d common to several simulations discussed in the literature (Eden, 2007; Eden et al., 2007; Eden and Greatbatch, 2008, 2009; Zhai and Greatbatch, 2006), is the presence of negative values in rather wide regions. In our simulations, we had not more than 20% instantaneous negative values of Eq. (14c), as shown in the histogram in Fig. 2d. However, after averaging over several months, negative κ_M^d were no longer present. Furthermore, the values of diagnosed and model diffusivities are rather close and their spatial correlations are about 0.5–0.65 for different simulations.

(b) Vertical flux and re-stratification

The vertical buoyancy flux is given by Eq. (9a,b) with $\tau=b$. Figure 4 shows the profiles of the basin and seasonally averaged simulated F_V^b and the one predicted by the model. They are quite similar and of the same sign and magnitude. Near the bottom of the ML, F_V^b has a minimum and then begins to grow again with depth. The second derivative of F_V^b is negative which leads to re-stratification of the ML.

4.2.2 Realistic flows

In Table 1 we present some of the features of typical flows and the results of diagnosed mesoscale horizontal and vertical fluxes and K at the center of the ML averaged over the basin over a three months period. As one can see from the Table, the correlation between the diagnosed mesoscale fluxes F_V^d and eddy kinetic energy K_d with their theoretical counterparts F_V^{th} and K_{th} is large; in all cases, the seasonally averaged horizontal diffusivities κ_M^d diagnosed using Eq. (14c) are positive and of the same order of magnitude as its theoretical κ_M^{th} diagnosed using the second Eq. (4h). In Fig. 5, we present the scatter plot of instantaneous diagnosed diffusivities κ_M^d vs. κ_M^{th} for three typical simulated flows, 1N, 2N and 4R. As one can see, the agreement is satisfactory, and the percentage of negative κ_M^d is rather low (10–25%). The profiles $F_V^d(z)$ and

Mixed layer mesoscales: a parameterization for OGCMs

V. M. Canuto et al.

Title Page

Abstract

Introduction

Conclusions

References

Tables

Figures

⏪

⏩

◀

▶

Back

Close

Full Screen / Esc

Printer-friendly Version

Interactive Discussion



$F_V^{\text{th}}(z)$ also are in satisfactory agreement and typical examples are presented in Fig. 6 (cases 8R, 6R and 1N).

4.2.3 Competition between small scale turbulent and mesoscale vertical fluxes

As Eq. (13) shows, vertical fluxes can either increase or decrease the ML stratification depending on the sign of the second z-derivative of the vertical fluxes. Small scale turbulent vertical fluxes are known to de-stratify the ML while we have shown that mesoscales do the opposite. It is therefore important to quantify their relative contributions. In Fig. 7 we show the mesoscale and small scale vertical fluxes, their first z-derivatives that enter in Eq. (1b) for the mean tracer field and their second z-derivatives that enter the time evolution of the stratification N^2 . As one can observe from any of the figures, turbulence and mesoscale vertical fluxes are almost the mirror image of each other and thus a large cancellation ensues. A less well mixed ocean's upper layer results with possibly important consequences for heat and CO_2 absorption that would be interesting to explore especially for their implications on climate studies.

5 Comparison of mesoscale and sub-mesoscale fluxes

For completeness we notice that the horizontal SM flux is smaller its mesoscale counterpart more than in order of magnitude. In fact, F_H^{SM} is parameterized analogously to Eq. (4h) with the substitution $\kappa_M \rightarrow \kappa_{\text{SM}} = r_s K_{\text{SM}}^{1/2}$, where r_s is defined in the last relation in Eq. (11b) in which h is the depth of the ML. Since r_d , which has a form similar to r_s but with H (ocean depth) in stead of h , is an order of magnitude larger than r_s and since the mesoscale kinetic energy is much larger than K_{SM} , one can neglect F_H^{SM} in comparison with its mesoscale counterpart.

As for the vertical SM and mesoscale fluxes, the situation is almost the reversed. To compare such fluxes, we notice that the shapes of their profiles are quite similar, which is clear by comparing the profiles in Figs. 6–7 for mesoscales with those for SM

Mixed layer mesoscales: a parameterization for OGCMs

V. M. Canuto et al.

Title Page

Abstract

Introduction

Conclusions

References

Tables

Figures



Back

Close

Full Screen / Esc

Printer-friendly Version

Interactive Discussion



**Mixed layer
mesoscales: a
parameterization for
OGCMs**

V. M. Canuto et al.

Title Page

Abstract

Introduction

Conclusions

References

Tables

Figures

⏪

⏩

◀

▶

Back

Close

Full Screen / Esc

Printer-friendly Version

Interactive Discussion



given in Fig. 2 of CD9 or Fig. 6a of Fox-Kemper and Ferrari (2008). This implies that it is sufficiently to compare any characteristic of the profiles, for example, the maximal values of the vertical fluxes or their z-derivatives at the surface. We chose the later characteristic since for SM in the case of a strong down-front wind, from Eqs. (8a) and (9a) of CD9 it is easy to derive the following simple formula for the SM buoyancy flux

$$z = 0: \partial_z F_V^{\text{SM}} \sim \eta 2^{1/2} (\delta_E f \rho)^{-1} |\tau| \left| \nabla_H \bar{b} \right| \quad (15a)$$

where δ_E is the thickness of the Ekman layer, ρ is the density of water, τ is the wind stress, and η is given in Eq. (11b). Consider, for example, the flow 8R described in Sect. 4.2.2 in Table 1. From Fig. 6a or Fig. 7 for the mesoscale buoyancy flux we obtain

$$z = 0: \partial_z F_V \approx 1.5 \times 10^{-9} \text{ ms}^{-3} \quad (15b)$$

To obtain the corresponding characteristic for SM, into Eq. (15a) we substitute $\delta_E \approx 10 \text{ m}$ together with $|\tau| = 0.1 \text{ Nm}^{-2}$ and $\nabla_H \bar{b} \approx 4 \cdot 10^{-8} \text{ s}^{-2}$ from Table 1. Since for the case of strong wind $\eta \lesssim 1$, from Eq. (15a) we get

$$z = 0: \partial_z F_V^{\text{SM}} \lesssim 5.7 \cdot 10^{-9} \text{ ms}^{-3} \quad (15c)$$

Thus, in the case of strong down-front wind, the SM vertical buoyancy flux is about five times larger than its mesoscale counterpart. In addition, in the case of no wind and only baroclinic instabilities, the ratio of any of the terms in Eq. (9) with Eq. (13b) of CD9 yields a ratio of the order of ten. Thus, we conclude that in general we have:

$$\frac{F_{\text{SM}}}{F_{\text{m}}} \approx 5 - 10 \quad (15d)$$

Does it mean that the parameterization of the mesoscale vertical flux is of no interest? The answer is negative since in such a case, as discussed by Mahadevan et al. (2010) and in CD9, there is a strong cancellation of the re-stratifying effect of SM

and the de-stratifying effect due to the mean flow, in which case the re-stratifying effect of mesoscale becomes important. In addition, in the case of a strong up-front wind, the SM parameterization in CD9 predicts that SM are not generated. If this prediction will be confirmed, then mesoscales remain the only factor of the re-stratification of the ML.

5 Finally, in any case the parameterization of the vertical mesoscale buoyancy flux is indispensable for a parameterization of the surface mesoscale kinetic energy that, together with the profile of $K(z)$, is necessary for a parameterization of the mesoscale diffusivity in accordance with Eq. (4h).

6 Conclusions

10 The horizontal, vertical fluxes and mesoscale kinetic energy were constructed using the solutions of the mesoscale dynamic equations with the inclusion of the non-linear terms. The model results, which render the tapering procedure unnecessary, can be used in coarse resolution OGCMs since they are expressed in terms of the resolved fields. It may be worth recalling some of the key features of the model:

- 15 (a) the vertical flux vanishes automatically at $z=0$ without additional requirements, and it is valid for an arbitrary diffusivity and arbitrary tracer,
- (b) the model predicts that mesoscales re-stratify the mixed layer, in agreement with existing simulation data,
- (c) the predicted surface mesoscale kinetic energy compares well the T/P data,
- 20 (d) in the presence of strong winds, the sub-mesoscale kinetic energy K_{SM} can exceed the baroclinic mean kinetic energy \tilde{K} defined in Eq. (11c). Thus, the mean Eulerian velocity \bar{u} that enters the mesoscale vertical flux given by Eq. (9a,b), is affected by the presence of sub-mesoscales which induce the change represented by Eq. (11f),

Mixed layer mesoscales: a parameterization for OGCMs

V. M. Canuto et al.

Title Page

Abstract

Introduction

Conclusions

References

Tables

Figures



Back

Close

Full Screen / Esc

Printer-friendly Version

Interactive Discussion



- (e) results of an eddy resolving simulation help to further assess the predictions of the model,
- (f) there is an interesting analogy between the deep ocean mesoscales that cancel much of the mean Eulerian velocity and the mixed layer mesoscales that also induce a cancellation: the vertical flux largely cancels the flux by small scale turbulence, implying a less well mixed layer. The implications of a more stratified mixed layer on the ocean's heat and CO₂ absorption have interesting implications on climate studies which will be pursued next.

Appendix A

Corrections to the mesoscale tracer field and the vertical tracer flux

Near the bottom of the ML the approximation (Eq. 3f) is not sufficient and one needs to add the term $w'\bar{\tau}_z$ to the left hand side of Eq. (2d). Then, instead of Eq. (3f), we have the following relation:

$$\tau' = -[\chi + ik \cdot (\bar{\mathbf{u}} - \mathbf{u}_d)]^{-1} (\mathbf{u}' \cdot \nabla_H \bar{\tau} + w'\bar{\tau}_z) \quad (\text{A1})$$

which results in the following additional term in the expression (Eq. 3f):

$$\delta\tau' = -[\chi + ik \cdot (\bar{\mathbf{u}} - \mathbf{u}_d)]^{-1} \bar{\tau}_z w' \quad (\text{A2})$$

With the help of this result, we carry out the procedure in Sect. 2.4 to compute the correction $\delta F_v \equiv \overline{\delta\tau' w'}$ first in \mathbf{k} -space and then in physical space. We obtain:

$$\delta F_v = -\chi^{-1} \overline{w'^2 \bar{\tau}_z} \quad (\text{A3})$$

To compute $\overline{w'^2}$, we use the first relation (Eq. 7a). To the leading order, this relation yields $w' = -iz\chi k f^{-1} u_g$ which, in turn yields:

$$\overline{w'^2} = 2 z^2 r_d^{-2} \chi^2 f^{-2} K \quad (\text{A4})$$

Mixed layer mesoscales: a parameterization for OGCMs

V. M. Canuto et al.

Title Page

Abstract

Introduction

Conclusions

References

Tables

Figures

⏪

⏩

◀

▶

Back

Close

Full Screen / Esc

Printer-friendly Version

Interactive Discussion



Substituting this result into Eq. (A3) and using $\chi \sim r_d^{-1} K^{1/2}$, we obtain Eq. (8c).

Appendix B

Correction to the mesoscale tracer equation due to sub-mesoscales

5 The model presented in the text was based on the splitting of an arbitrary variable A as follows:

$$A = \bar{A} + A' + A^t \quad (\text{B1})$$

where a prime represents the mesoscale fields, t stands for turbulence giving rise to the F^{SS} flux in Eq. (1b) and an overbar stands for averages over large scales. However, 10 as we discussed in the Introduction, the increased horizontal resolution up to a few kilometers and even smaller, achieved in recent simulations has shown that Eq. (B1) may not be sufficient for a full representation of sub-grid processes in the ML. The reason is that the vertical flux of sub-mesoscales (SM; ≤ 1 km), which are intermediate between mesoscale and turbulence scales, has a strong effect on the ML dynamics. 15 A model for SM was recently presented (Canuto and Dubovikov, 2009, CD9) and its extension so as to make it applicable in coarse resolution OGCM has recently been completed (Canuto and Dubovikov, 2010). Such an effect is quite distinct from that of small scales since the latter lead to de-stratification while the SM re-stratify the ML (Hosegood et al., 2008). For this reason, the effect of SM cannot be lumped together 20 with that of small scale turbulence. Thus, at least in the ML, instead of Eq. (B1) one must use the decomposition:

$$A = \bar{A} + A' + A'' + A^t \quad (\text{B2})$$

where A'' now denotes SM fields. Correspondingly, instead of Eq. (1b), the tracer equation is now as follows:

$$25 \partial_t \bar{\tau} + \bar{\mathbf{U}} \cdot \nabla \bar{\tau} + \nabla \cdot \mathbf{F}^m + \partial_z F_V^{\text{SM}} + \partial_z F_V^{\text{SS}} = \bar{G} \quad (\text{B3})$$

where $F^{\text{SM}} = \overline{U''\tau''}$ is the SM tracer flux of which we consider only the vertical component. We begin with the tracer equation averaged over scales smaller than mesoscales but larger than submesoscales. Denoting the averaged fields by $\overline{\overline{A}}$, from Eqs. (B1,2) we have:

$$\overline{\overline{A}} = \overline{A} + A' \quad (\text{B4})$$

The equation for $\overline{\overline{\tau}}$ is obtained by analogy with Eq. (1b) to be:

$$\partial_t \overline{\overline{\tau}} + \overline{\overline{U}} \cdot \nabla \overline{\overline{\tau}} + \partial_z \overline{\overline{F_V^{\text{SM}}}} = \partial_z (k_v \overline{\overline{\tau}}_z) + G \quad (\text{B5})$$

where we have accounted for only the contribution of the vertical components of the sub-mesoscale and small scale turbulent fluxes and parameterized the latter in the form of a vertical diffusion. In a previous paper (Canuto and Dubovikov, 2009, CD9) we parameterized the sub-mesoscale contribution in Eq. (B5) in terms of resolved fields $\overline{\overline{A}}$ using the notation \overline{A} for the latter. The result is given by Eq. (7a) of CD9 which we rewrite below in the present notation:

$$\partial_z \overline{\overline{F_V^{\text{S}}}} = \mathbf{u}_S^+ \cdot \nabla_H \overline{\overline{\tau}} \quad (\text{B6})$$

where \mathbf{u}_S^+ is expressed by relations (Eq. 11a,b) with:

$$\tilde{\mathbf{u}} = \overline{\overline{\mathbf{u}}} - \langle \overline{\overline{\mathbf{u}}} \rangle, \tilde{K} = \frac{1}{2} |\tilde{\mathbf{u}}|^2, \langle \overline{\overline{\mathbf{u}}} \rangle = h^{-1} \int_{-h}^0 \overline{\overline{\mathbf{u}}}(z) dz \quad (\text{B7})$$

and K_S is expressed in terms of resolved fields in Eq. (7j,k) of CD9 which we rewrite below in the present notation:

$$K_S^{3/2} = 2 C^{3/2} r_S h \eta (\tilde{\mathbf{V}} - \lambda \mathbf{e}_z \times \tilde{\mathbf{V}}) \cdot \nabla_H \overline{\overline{b}}, \tilde{\mathbf{V}} = -\frac{1}{2} \langle \overline{\overline{\mathbf{u}}} \rangle - h^{-2} \int_{-h}^0 dz \int_0^z \overline{\overline{\mathbf{u}}}(z') dz' \quad (\text{B8})$$

Mixed layer mesoscales: a parameterization for OGCMs

V. M. Canuto et al.

Title Page	
Abstract	Introduction
Conclusions	References
Tables	Figures
◀	▶
◀	▶
Back	Close
Full Screen / Esc	
Printer-friendly Version	
Interactive Discussion	



From Eq. (B7) it follows that $\overline{\langle \tilde{\mathbf{u}} \rangle}$ is the barotropic component of the resolved velocity $\overline{\mathbf{u}} = \overline{\mathbf{u}} + \mathbf{u}'$ within the ML while $\tilde{\mathbf{u}}$ is the baroclinic one which in the case of a strong wind, is contributed mostly by the baroclinic component of $\overline{\mathbf{u}}$ since the mesoscale velocity field \mathbf{u}' is almost barotropic within the ML (see, for example, Capet et al., 2008, Fig. 10).

5 Therefore, substituting $\overline{\mathbf{u}} = \overline{\mathbf{u}} + \mathbf{u}'$ in Eq. (B7), we may neglect the contribution of \mathbf{u}' that results in Eq. (11c). From the definition of $\overline{\langle \tilde{\mathbf{u}} \rangle}$ in Eq. (B7), it follows that $\tilde{\mathbf{V}}$ in Eq. (B8) may be rewritten in the form:

$$\tilde{\mathbf{V}} = -h^{-2} \int_{-h}^0 dz \left(\int_0^z \tilde{\mathbf{u}}(z') dz' \right) \quad (\text{B9})$$

10 Therefore, we may neglect the contribution of \mathbf{u}' in both definitions of $\tilde{\mathbf{V}}$, Eqs. (B9) and (B8), that transforms Eq. (B8) into Eq. (11e) with $\tilde{\mathbf{u}}$ given in Eq. (11c). Finally, dividing Eq. (B8) by $\tilde{K}^{3/2}$ and using notations (Eq. 11b), we obtain Eq. (11d).

References

- Blumberg, A. F. and Mellor, G. L.: A description of a three-dimensional coastal ocean circulation model, Three-Dimensional Coastal Ocean Models, edited by: Heaps, N. S., Amer. Geophys. Union, 1987.
- 15 Canuto, V. M. and Dubovikov, M. S.: A new approach to turbulence, *Int. J. Mod. Phys.*, 12, 3121–3152, 1997.
- Canuto, V. M. and Dubovikov, M. S.: Modeling mesoscale eddies, cited as CD5, *Ocean Model.*, 8(1), 30, 2005
- 20 Canuto, V. M. and Dubovikov, M. S.: Dynamical model of mesoscales in z-coordinates, cited as CD6, *Ocean Model.*, 11, 123–166, 2006.
- Canuto, V. M. and Dubovikov, M. S.: Derivation and assessment of a mixed layer sub-mesoscale model, *Ocean Sci. Discuss.*, 6, 2157–2192, 2009, <http://www.ocean-sci-discuss.net/6/2157/2009/>.

Mixed layer mesoscales: a parameterization for OGCMs

V. M. Canuto et al.

Title Page

Abstract

Introduction

Conclusions

References

Tables

Figures

⏪

⏩

◀

▶

Back

Close

Full Screen / Esc

Printer-friendly Version

Interactive Discussion



**Mixed layer
mesoscales: a
parameterization for
OGCMs**

V. M. Canuto et al.

Title Page

Abstract

Introduction

Conclusions

References

Tables

Figures

⏪

⏩

◀

▶

Back

Close

Full Screen / Esc

Printer-friendly Version

Interactive Discussion



- Canuto, V. M. and Dubovikov, M. S.: Sub-Mesoscale model for coarse resolution OGCMs, *Ocean Sci.*, to be submitted, 2010.
- Canuto, V. M., Howard, A. M., Cheng, Y., Muller, C. J., Leboissetier, A., and Jayne, S. R.: *Ocean Turbulence III: New GISS vertical mixing scheme*, *Ocean Model.*, in press, 2010.
- 5 Capet, X., McWilliams, J. C., Molemaker, M. J., and Shchepetkin, A. F.: Mesoscale to sub-mesoscale transition in the California current system, Part I: flow structure, eddy flux, and observational tests, *J. Phys. Oceanogr.*, **38**, 29–43, 2008.
- Choi, J. K., Kantha, L. H., and Leben, R. R.: A nowcast/forecast experiment using TOPEX/POSEIDON and ERS-1 altimetric data assimilation into a three-dimensional circulation model of the Gulf of Mexico, IAPSO Abstract, 21st General Assembly of the International Union of Geodesy and Geophysics, Boulder, CO, International Union of Geodesy and Geophysics, B324, 1995.
- 10 Clayson, C. A.: Modeling the mixed layer in the tropical Pacific Ocean and air-sea interactions: Application to a westerly wind burst. Ph.D. Dissertation, University of Colorado, available from University of Colorado Libraries, Campus Box 184, University of Colorado, Boulder, CO 80309-0184, 174 pp., 1995.
- Clayson, C. A. and Luneva, M.: Deep convection in the Japan (East) Sea: A model perspective, *Geophys. Res. Lett.*, **31**, L17303, doi:10.1029/2004GL020497, 2004.
- Clayson, C. A., Luneva, M., and Cunningham, P.: Downwelling and upwelling and regimes: Connection between surface fronts and abyssal circulation, *Dynamics of Atmospheres and Oceans, Special Issues on Processes at Oceanic Fronts*, 2008.
- 20 Clifford, M., Horton, C., Schmitz, J., and Kantha, L.: 1997, An oceanographic nowcast/forecast system for the Red Sea, *J. Geophys. Res.*, **102**, 25 1997.
- Eden, C.: Eddy length scales in the North Atlantic, *J. Geophys. Res.*, **112**, C06004, doi:10.1029/2006JC003901, 2007.
- 25 Eden, C. and Greatbatch, R. J.: Toward a mesoscale eddy closure, *Ocean Model.*, **20**, 223–239, 2008.
- Eden, C., Greatbatch, R. J., and Willebrand, J.: A diagnosis of thickness fluxes in a eddy-resolving model, *J. Phys. Oceanogr.*, **37**, 727–742, 2007.
- 30 Eden, C. and Greatbatch, R. J.: A diagnosis of isopycnal mixing by mesoscale eddies, *Ocean Model.*, **27**(1–2) 98–106, 2009.

Mixed layer mesoscales: a parameterization for OGCMs

V. M. Canuto et al.

Title Page

Abstract

Introduction

Conclusions

References

Tables

Figures

⏪

⏩

◀

▶

Back

Close

Full Screen / Esc

Printer-friendly Version

Interactive Discussion



- Engelhardt, D. B.: Estimation of North Pacific Ocean dynamics and heat transport from TOPEX/POSEIDON satellite altimetry and a primitive equation ocean model. Ph.D. Dissertation, University of Colorado, available from University of Colorado Libraries, Campus Box 184, University of Colorado, Boulder, CO 80309-0184, 132 pp., 1996.
- 5 Ferrari, R., McWilliams, J. C., Canuto, V. M., and Dubovikov, M.: Parameterization of Eddy Fluxes near Oceanic Boundaries, *J. of Climate*, 21, 2770–2789, 2008.
- Fox-Kemper, B. and Ferrari, R.: Parameterization of mixed layer eddies, Part II: prognosis and impact, *J. Phys. Oceanogr.*, 38, 1166–1179, 2008.
- Gent, P. R. and McWilliams, J. C.: Isopycnal mixing in ocean circulation models, *J. Phys. Oceanogr.*, 20, 150–155, 1990.
- 10 Horton, C., Clifford, M., Cole, D., Schmitz, J., and Kantha, L.: Water circulation modeling system for the Persian Gulf, Proc. 1991 Marine Technology Society Meeting, New Orleans, LA, Marine Technology Society, 557–560, 1991.
- Horton, C., Clifford, M., Cole, D., Schmitz, J., and Kantha, L.: Operational modeling: Semi-enclosed basin modeling at the Naval Oceanographic Office, *Oceanography*, 6, 69–72, 1992.
- 15 Horton, C., Clifford, M., Schmitz, J., and Kantha, L.: A real-time oceanographic now-cast/forecast system for the Mediterranean Sea, *J. Geophys. Res.*, 102, 25, 1997.
- Hosegood, P. J., Gregg, M. C., and Alford, M. H.: Restratification of the Surface Mixed Layer with Submesoscale Lateral Density Gradients: Diagnosing the importance of the horizontal dimension, *J. Phys. Oceanogr.*, 38, 2438–2460, 2008.
- 20 Kantha, L. H.: Monitoring the oceans using data-assimilative models: Implications for integrated in-situ and remote observing systems, Abstract, Third Symp. on Integrated Observing Systems, Dallas, TX, Am. Meteor. Soc., 183–188, 1999.
- 25 Kantha, L. H.: On an improved model of the turbulent PLB., *J. Atmos. Sci.*, 60, 2239–2246, 2003.
- Kantha, L. H. and Piacsek, S.: Ocean models, Computational Science Education Project, edited by: Meiser, V., Department of Energy, 273–361, 1993.
- Kantha, L. H. and Clayson, C. A.: An improved mixed layer model for geophysical applications, *J. Geophys. Res.*, 99, 25, 1994.
- 30 Kantha, L. H. and Piacsek, S.: Computational Ocean Modeling, Handbook for Computer Science and Engineering, edited by: Tucker, A., CRC Press, 934–958, 1997.

Mixed layer mesoscales: a parameterization for OGCMs

V. M. Canuto et al.

Title Page

Abstract

Introduction

Conclusions

References

Tables

Figures

◀

▶

◀

▶

Back

Close

Full Screen / Esc

Printer-friendly Version

Interactive Discussion



- Kantha, L. H. and Clayson, C. A.: Numerical models of oceans and oceanic processes, Academic Press, 2000.
- Killworth, P. D.: On parameterization of eddy transport, *J. Mar. Res.*, 55, 1171–1197, 1997.
- Killworth, P. D.: Boundary conditions on quasi-Stokes velocities in parameterizations, *J. Phys. Oceanogr.*, 31, 1132–1155, 2001.
- 5 Killworth, P. D.: Parameterization of eddy effect on mixed layer tracer transport: a linearized eddy perspective, *J. Phys. Oceanogr.*, 35, 1717–1725, 2005.
- Klein, P., Hua, B. L., Lapeyre, G., Capet, X., Le Gentil, S., and Sasaki, H.: Upper ocean turbulence from high resolution 3D simulation, *J. Phys. Oceanogr.*, 38, 1748–1763, 2008.
- 10 Large, W. G., Danabasoglu, G., Doney, S. C., and McWilliams, J. C.: Sensitivity to surface forcing and boundary layer mixing in a global ocean model: Annual-Mean climatology, *J. Phys. Oceanogr.*, 27, 2418–2447, 1997.
- Ledwell, J. R., Watson, A. J., and Law, C. S.: Evidence for slow mixing across the pycnocline from open ocean tracer release experiment, *Nature*, 364, 701–703, 1993.
- 15 Lee, D.-K. and Niiler, P. P.: The energetic surface circulation patterns of the Japan/East Sea, *Deep-Sea Res. Pt. II*, 52, 1547–1563, 2005.
- Lesieur, M.: *Turbulence in Fluids*, Kluwer, Dordrecht, 212 pp. (Sect. 3.3), 1990.
- Levy, M., Klein, P., and Treguier, A. M.: Impacts of sub-mesoscale physics on production and subduction of phytoplankton in an oligotrophic regime, *J. Mar. Res.*, 59, 535–565, 2001.
- 20 Levy, M., Klein, P., Treguier, A. M., Iovino, D., Madec, G., Masson, S., and Takahashi, K.: Modification of gyre circulation by submesoscale physics, *Ocean Model.*, in press, 2009.
- Lopez, J. W.: A data-assimilative model of the North Indian Ocean. Doctoral dissertation, University of Colorado, available from University of Colorado Libraries, Campus Box 184, University of Colorado, Boulder, CO 80309-0184, 152 pp., 1998.
- 25 Lopez, J. W. and Kantha, L. H.: Results from a numerical model of the northern Indian Ocean: Circulation in the South Arabian Sea, *J. Mar. Syst.*, 24, 97–117, 2000.
- Luneva, M. and Clayson, C. A.: Connection between surface fluxes and deep circulations in the Sea of Japan, *Geophys. Res. Lett.*, 33, L24602, doi:10.1029/2006GL027350, 2006.
- Mahadevan, A.: Modeling vertical motion at ocean fronts: Are non-hydrostatic effects relevant to sub-mesoscales?, *Ocean Model.*, 14, 222–240, 2006.
- 30 Mahadevan, A. and Tandon, A.: An analysis of mechanisms for sub-mesoscale vertical motion at ocean fronts, *Ocean Model.*, 14, 241–256, 2006.

Mixed layer mesoscales: a parameterization for OGCMs

V. M. Canuto et al.

Title Page

Abstract

Introduction

Conclusions

References

Tables

Figures

⏪

⏩

◀

▶

Back

Close

Full Screen / Esc

Printer-friendly Version

Interactive Discussion



Mahadevan, A., Tandon, A., and Ferrari, F.: Rapid changes in mixed layer stratification driven by sub-mesoscales instabilities and winds, *J. Geophys. Res.*, 115, C03017, doi:10.1029/2008JC005203, 2010.

Oschlies, A.: Improved representation of upper-ocean dynamics and mixed layer depths in a model of the North Atlantic on switching from eddy-permitting to eddy resolving grid resolution, *J. Phys. Oceanogr.*, 32, 2277–2298, 2002.

Richardson, P. L.: Tracking ocean eddies, *Am. Sci.*, 81, 261–271, 1993

Scharffenberg, M. G. and Stammer, D.: Seasonal variations of the geostrophic flow field and of eddy kinetic energy inferred from TOPEX/POSEIDON and Jason-1 Tandem Mission Data, *J. Geophys. Res.*, 115, C02008, doi:10.1029/2008JC005242, 2010.

Suk, M.-S., and Kantha, L. H.: Numerical studies of the East Sea (Sea of Japan), The Second CREAMS International Symposium, Fukuoka, Japan, North Pacific Marine Science Organization and University of Washington, 93–96, 1997.

Takematsu, M., Nagano, Z., Ostrovskii, A. G., Kim, K., and Volkov, Y.: Direct Measurements of Deep Currents in the Northern Japan Sea, *J. Oceanogr.*, 55, 207–216, 1999.

Thomas, L. N. and Lee, C. M.: Intensification of ocean fronts by down-front winds, *J. Phys. Oceanogr.*, 35, 1086–1102, 2005.

Thomas, L. N., Tandon, A., and Mahadevan, A.: Submesoscale processes and dynamics, in: *Eddy Resolving Ocean Modeling*, edited by: Hecht, M. and Hasumi, H., AGU Monograph, American Geophysical Union, Washington, DC, 17–38 pp., 2008.

Toole, J. M., Polzin, K. L., and Schmitt, R. W.: Estimates of diapycnal mixing in the abyssal ocean, *Science*, 264, 1120–1123, 1994.

Treguier, A. M., Held, I. M., and Larichev, V. D.: Parameterization of quasi geostrophic eddies in primitive equation ocean models, *J. Phys. Oceanogr.*, 27, 567–580, 1997.

Zhai, X. and Greatbatch, R. J.: Inferring the eddy-induced diffusivity for heat in the surface mixed layer using satellite data, *Geophys. Res. Lett.*, 33, L24607, doi:10.1029/2006DL027875, 2006.

Zhurbas, V., and Oh, I. S.: Lateral diffusivity and Lagrangean scales in the Pacific Ocean as derived from drifter data, *J. Geophys. Res.*, 108(C5), 3141, doi:10.1029/2002JC001596, 2003.

Mixed layer mesoscales: a parameterization for OGCMs

V. M. Canuto et al.

Table 1. The first five rows correspond to the wind stresses, heat losses, Rossby radii, horizontal mean buoyancy gradient and mixed layer depth characterizing the different simulations represented by the letters N and R. The remaining rows represent the values (in the middle in the mixed layer) of the simulated (d, for diagnosed) and model (th, for theoretical) vertical buoyancy flux, eddy kinetic energy and mesoscale diffusivity.

	1N	2N	4R	5R	7R	8R	9R	10R
τ/τ_0	0.5	1	0.5	1	2	0.5	1	1.5
$Q_b \text{ W m}^{-2}$	130	130	130	130	0	0	0	0
$r_d \text{ km}$	15.3	13	16	13	10	19	15.4	12.6
$10^8 \nabla_{\text{Hb}}^- \text{ s}^{-2}$	3.4	6.4	3.4	6.5	2.7	3.8	3.0	2.7
$h \text{ m}$	137	182	141	184	277	88	141	185
$10^8 F_V^d \text{ m}^2 \text{ s}^{-3}$	3.2	5.5	5.4	4.8	3.9	3.5	4.4	3.2
$10^8 F_V^{\text{th}} \text{ m}^2 \text{ s}^{-3}$	3.1	4.1	5.0	5.6	5.4	2.7	3.2	3.9
$\text{Corr } F_V$	0.5	0.7	0.7	0.4	0.7	0.4	0.6	0.8
$10^2 K_d \text{ m}^2 \text{ s}^{-2}$	2.2	1.7	3.1	1.7	0.9	2.5	1.6	0.9
$10^2 K_{\text{th}} \text{ m}^2 \text{ s}^{-2}$	2	1.6	2.1	1.9	1.6	1.4	1.5	1.5
$\text{Corr } K$	0.4	0.2	0.3	0.2	0.5	0.6	0.5	0.75
$10^{-3} \kappa_M^d \text{ m}^2 \text{ s}^{-1}$	1.94	1.1	1.1	0.9	0.7	1.1	1.1	0.75
$10^{-3} \kappa_M^{\text{th}} \text{ m}^2 \text{ s}^{-1}$	2.3	1.7	2.8	1.7	0.9	3.0	1.9	1.1

Title Page

Abstract

Introduction

Conclusions

References

Tables

Figures

◀

▶

◀

▶

Back

Close

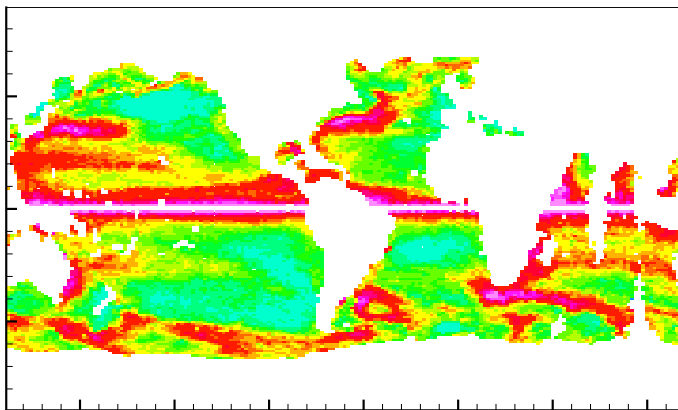
Full Screen / Esc

Printer-friendly Version

Interactive Discussion



Data (Scharffenberg and Stammer, 2009)



Model

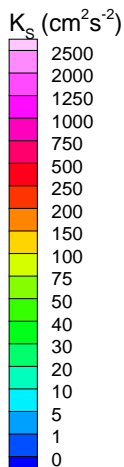
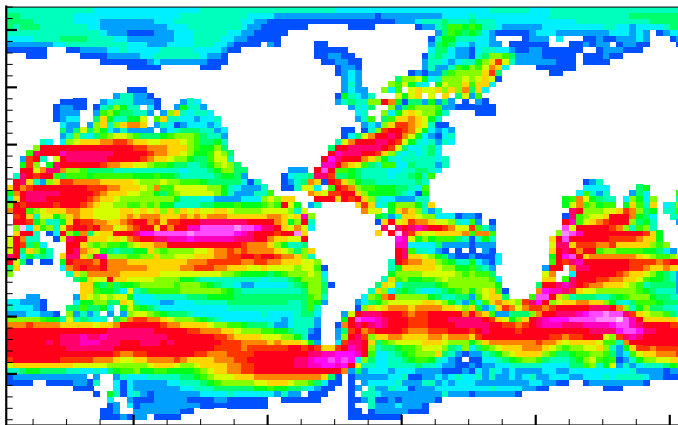


Fig. 1. Surface eddy kinetic energy K_s , Eqs. (10c–d), averaged over 3 years: **(a)** observational data from Scharffenberg and Stammer (2009) and **(b)** present model with the large fields computed from an OGCM.

Mixed layer mesoscales: a parameterization for OGCMs

V. M. Canuto et al.

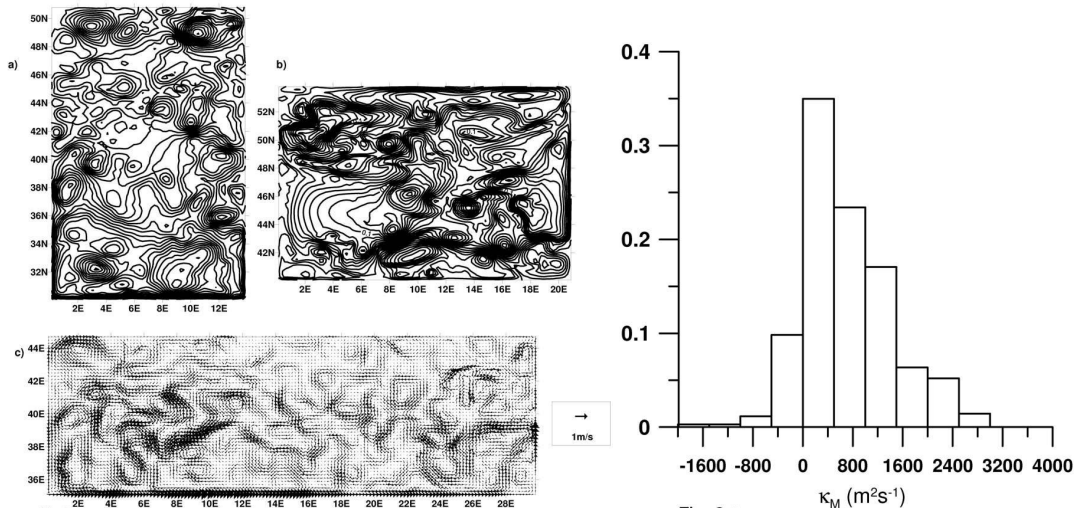


Fig. 2. (a)–(c) Idealized flows. Simulated snapshots of sea surface heights (contour interval is 2 cm) and velocity field at the 390th day in different basins. (d) Idealized flows. Typical histogram (in %) for the diagnosed instantaneous horizontal diffusivity.

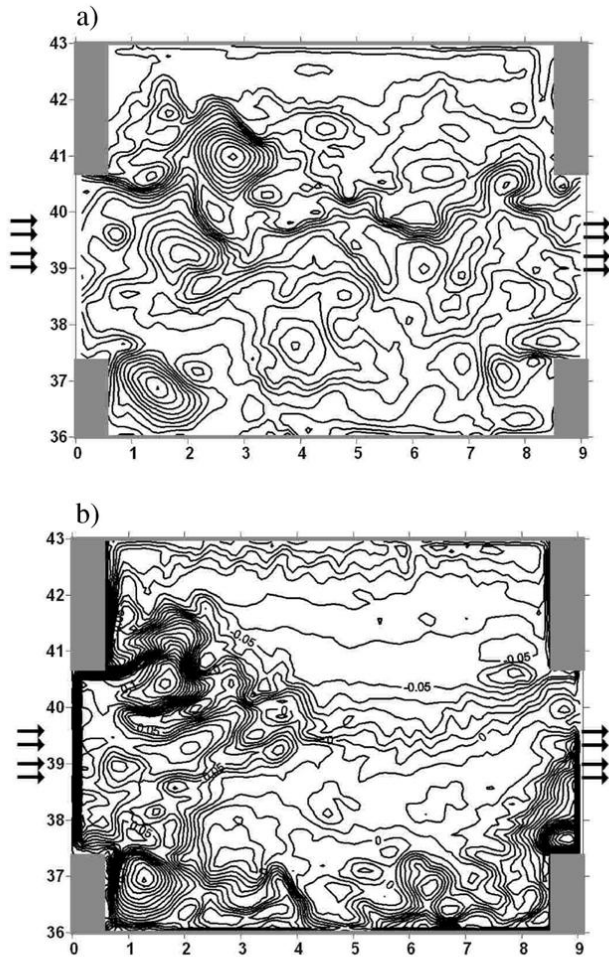


Fig. 3. Realistic flow. Snapshots of sea surface heights in different simulations.

Mixed layer mesoscales: a parameterization for OGCMs

V. M. Canuto et al.

Title Page

Abstract Introduction

Conclusions References

Tables Figures

⏪ ⏩

◀ ▶

Back Close

Full Screen / Esc

Printer-friendly Version

Interactive Discussion



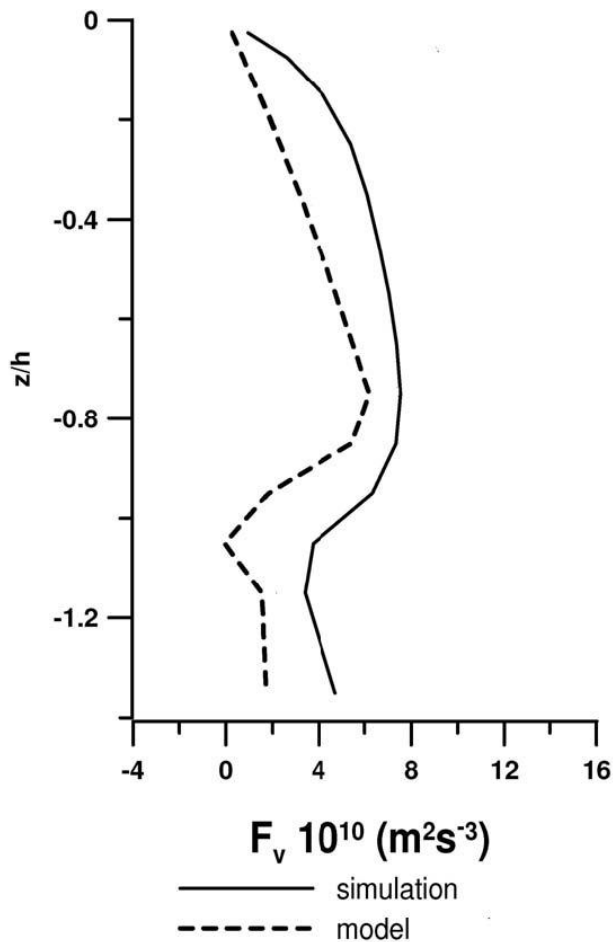


Fig. 4. Idealized flows. z -profiles of the model and simulation vertical buoyancy flux averaged seasonally and over the basin area; h is the mixed layer depth.

Mixed layer mesoscales: a parameterization for OGCMs

V. M. Canuto et al.

Title Page

Abstract Introduction

Conclusions References

Tables Figures

⏪ ⏩

◀ ▶

Back Close

Full Screen / Esc

Printer-friendly Version

Interactive Discussion



**Mixed layer
mesoscales: a
parameterization for
OGCMs**

V. M. Canuto et al.

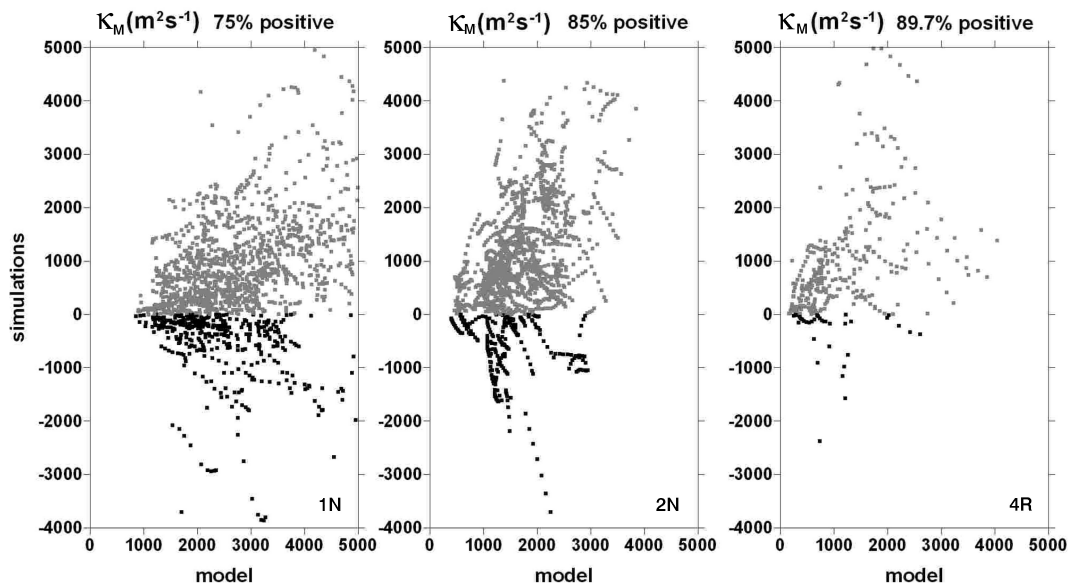


Fig. 5. Realistic flow. Scatter plots of diagnosed instantaneous horizontal diffusivities vs. model results in simulations 1N, 2N, 4R (see Table 1 for details of the simulations).

Title Page

Abstract

Introduction

Conclusions

References

Tables

Figures

◀

▶

◀

▶

Back

Close

Full Screen / Esc

Printer-friendly Version

Interactive Discussion

Mixed layer mesoscales: a parameterization for OGCMs

V. M. Canuto et al.

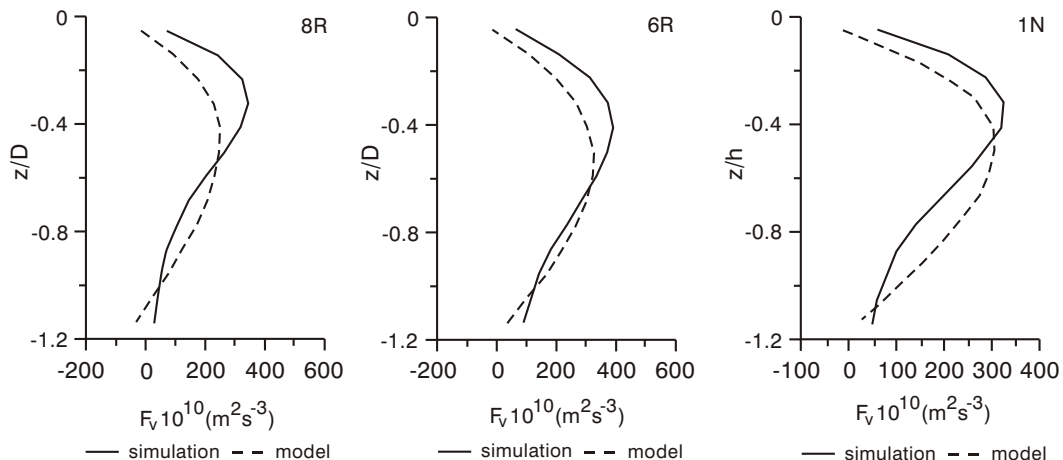


Fig. 6. Realistic flow. Profiles of the model and simulation vertical buoyancy flux averaged seasonably and over the basin area in simulations 8R, 6R and 1N (see Table 1 for details on the different cases).

Title Page

Abstract

Introduction

Conclusions

References

Tables

Figures

⏪

⏩

◀

▶

Back

Close

Full Screen / Esc

Printer-friendly Version

Interactive Discussion

Mixed layer mesoscales: a parameterization for OGCMs

V. M. Canuto et al.

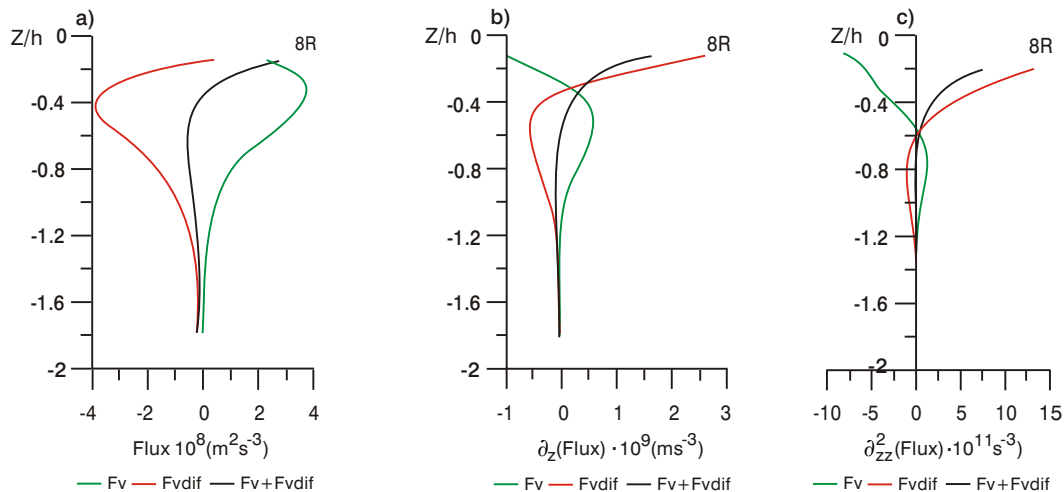


Fig. 7. Realistic flow. Mesoscale and small scale vertical buoyancy fluxes and their first and second z -derivatives.

[Title Page](#)
[Abstract](#)
[Introduction](#)
[Conclusions](#)
[References](#)
[Tables](#)
[Figures](#)
[⏪](#)
[⏩](#)
[◀](#)
[▶](#)
[Back](#)
[Close](#)
[Full Screen / Esc](#)
[Printer-friendly Version](#)
[Interactive Discussion](#)